



Design, synthesis, and evaluation of novel VEGFR2 kinase inhibitors: Discovery of [1,2,4]triazolo[1,5-*a*]pyridine derivatives with slow dissociation kinetics

Yuya Oguro*, Douglas R. Cary, Naoki Miyamoto, Michiko Tawada, Hidehisa Iwata, Hiroshi Miki, Akira Hori, Shinichi Imamura

Pharmaceutical Research Division, Takeda Pharmaceutical Company, Ltd, 2-26-1 Muraoka-higashi, Fujisawa, Kanagawa 251-8555, Japan

ARTICLE INFO

Article history:

Received 19 February 2013

Revised 12 April 2013

Accepted 13 April 2013

Available online 23 April 2013

Keywords:

Type-II VEGFR2 kinase inhibitor

PDGFR

[1,2,4]Triazolo[1,5-*a*]pyridine

ABSTRACT

For the purpose of discovering novel type-II inhibitors of vascular endothelial growth factor receptor 2 (VEGFR2) kinase, we designed and synthesized 5,6-fused heterocyclic compounds bearing an anilide group. A co-crystal structure analysis of imidazo[1,2-*b*]pyridazine derivative **2** with VEGFR2 revealed that the N1-nitrogen of imidazo[1,2-*b*]pyridazine core interacts with the backbone NH group of Cys919. To retain this essential interaction, we designed a series of imidazo[1,2-*a*]pyridine, [1,2,4]triazolo[1,5-*a*]pyridine, thiazolo[5,4-*b*]pyridine, and 1,3-benzothiazole derivatives maintaining a ring nitrogen as hydrogen bond acceptor (HBA) at the corresponding position. All compounds thus designed displayed strong inhibitory activity against VEGFR2 kinase, and the [1,2,4]triazolo[1,5-*a*]pyridine **13d** displayed favorable physicochemical properties. Furthermore, **13d** inhibited VEGFR2 kinase with slow dissociation kinetics and also inhibited platelet-derived growth factor receptor (PDGFR) kinases. Oral administration of **13d** showed potent anti-tumor efficacy in DU145 and A549 xenograft models in nude mice.

© 2013 Elsevier Ltd. All rights reserved.

1. Introduction

Angiogenesis, the formation of new blood vessels, plays important roles in the growth and metastasis of solid tumors.¹ It is generally thought that angiogenesis is required for the expansion of tumor mass beyond a certain size to supply oxygen and nutrients. Inhibition of tumor angiogenesis, therefore, has thus been targeted as a rational approach for anticancer therapy.²

Tumor angiogenesis is regulated by various kinds of angiogenesis factors. Vascular endothelial growth factors (VEGF) play a major role in tumor angiogenesis.³ VEGF induction in tumor cells can result from cancer-related changes including proto-oncogene activation,⁴ loss of tumor suppressor function,^{5,6} growth factor stimuli,⁷ and hypoxic status.^{8,9} The high-affinity VEGF receptors (VEGFR) consist of FLT1 (Fms-like tyrosine kinase 1; VEGFR1), KDR (VEGFR2), and FLT4 (VEGFR3).^{10–12} Binding of VEGF with VEGFR specifically exerts mitogenic and chemotactic activity on endothelial or lymphendothelial cells via receptor dimerization, leading to autophosphorylation of tyrosine residues in the intracellular kinase domain.¹³ Overactivation of VEGFR signaling positively correlates with poor prognosis and metastasis in the majority of solid tumor patients.^{14,15}

Therefore, abrogation of angiogenesis by VEGFR inhibition is regarded as a promising approach for the treatment of cancer. Indeed, several VEGFR kinase inhibitors (sunitinib,¹⁶ sorafenib,¹⁷ pazopanib,¹⁸ axitinib,¹⁹ and regorafenib²⁰) have been approved for various types of cancer, such as renal cell carcinomas.

Except for allosteric inhibitors, the majority of known kinase inhibitors are classified as type-I or type-II kinase inhibitors by their mode of binding with the target kinase.²¹ Although both type of inhibitors bind in and around the region occupied by the adenine ring of ATP, type-II kinase inhibitors induce the inactive conformation of kinases, enabling them to interact with a deeper region called the back pocket. Type-II kinase inhibitors have sev-

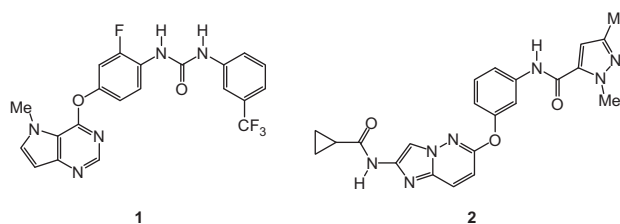


Figure 1. Pyrrolo[3,2-*d*]pyrimidine derivative **1** and imidazo[1,2-*b*]pyridazine derivative **2**.

* Corresponding author. Tel.: +81 466 32 1180; fax: +81 466 29 4458.

E-mail address: yuya.ooguro@takeda.com (Y. Oguro).

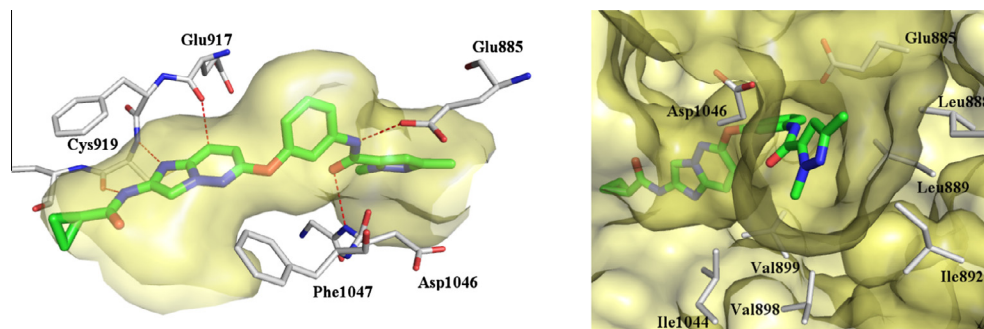


Figure 2. X-ray crystal structure of **2** bound to VEGFR2 (PDB ID 3VO3).

eral advantages over type-I kinase inhibitors such as slow off-rate profiles.^{22,23} We previously reported the urea-possessing pyrrolo[3,2-*d*]pyrimidine derivatives as type-II VEGFR2 kinase inhibitors.²⁴ The representative compound **1** (Fig. 1) inhibited VEGFR2 with slow dissociation kinetics and demonstrated potent inhibition of tumor growth in a DU145 human prostate cancer cell xenograft model in nude mice without serious toxicity. In our recent efforts to identify novel VEGFR2 kinase inhibitors, we also discovered the imidazo[1,2-*b*]pyridazine **2** (Fig. 1) as another type-II inhibitor of VEGFR2 kinase (VEGFR2 IC_{50} = 1.4 nM).²⁵ The crystal structure of the complex between **2** and VEGFR2 is shown in Figure 2. The kinase adopted an inactive conformation (DFG-out) so that the pyrazole-5-yl amide moiety occupies a hydrophobic back pocket. When compound **2** binds with VEGFR2, the N1-nitrogen of the imidazo[1,2-*b*]pyridazine core and the NH group of the cyclopropylamide at the 2-position interact with the backbone NH group and carbonyl of Cys919, respectively. CH \cdots O interaction is also observed between the 8-position of the imidazo[1,2-*b*]pyridazine

and the backbone carbonyl group of Glu917. The amide group between central benzene ring and pyrazole ring interacts with the protein through two hydrogen bonds; the amide proton forms a hydrogen bond with the side chain of Glu885 and the carbonyl interacts with the main chain of Asp1046. The external pyrazole moiety occupies the hydrophobic pocket created by the rearrangement of protein.

Based on this information, we expanded our investigation into different 5,6-fused heterocyclic ring systems to discover novel hinge-binding templates for type-II inhibitors of VEGFR2 kinase. As part of our strategy, the imidazo[1,2-*b*]pyridazine scaffold was replaced with other 5,6-fused heterocycles possessing a ring nitrogen as hydrogen bond acceptor (HBA) at the position corresponding to the N1-nitrogen of **2** so that the compounds could retain the essential hydrogen-bonding interaction with the main chain of Cys919 (Fig. 3(a)). Among the possible structures that meet this requirement, we reasoned that compounds possessing [1,2,4]triazolo[1,5-*a*]pyridine (**A**), imidazo[1,2-*a*]pyridine (**B**),

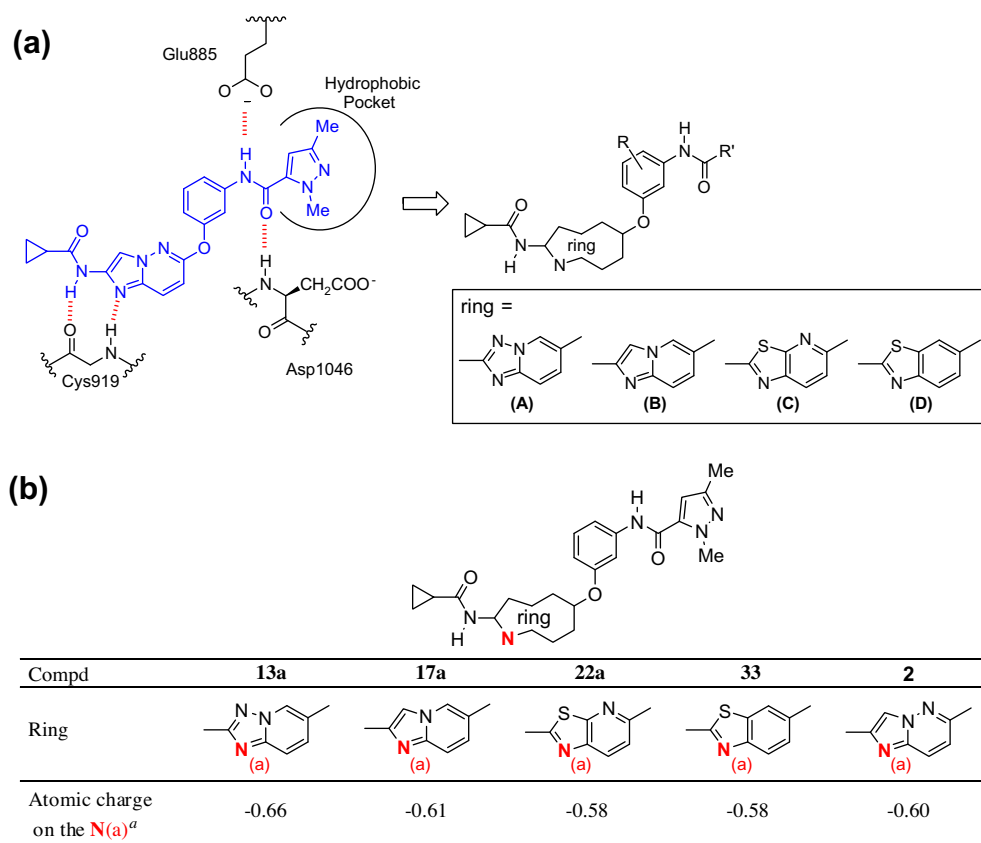


Figure 3. (a) Inhibitor Design. (b) Atomic charges of the representative compounds. ^aAtomic charges were calculated at the Hartree-Fock 6-31G* level using the Gaussian03.

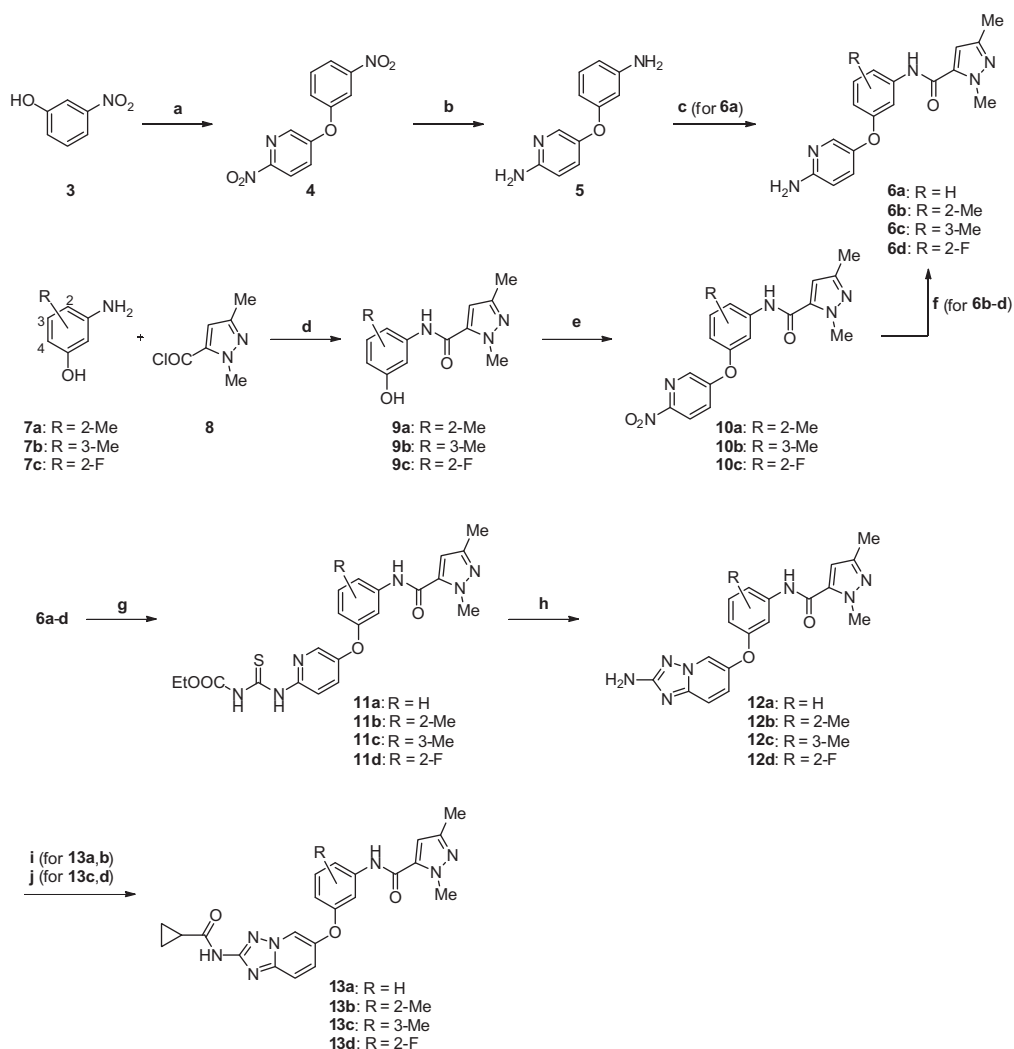
thiazolo[5,4-*b*]pyridine (**C**), and 1,3-benzothiazole (**D**) scaffolds might have good potential based on consideration of the atomic charge on nitrogen N(a) (Fig. 3(b)). Calculation of atomic charges revealed that the nitrogen atom (N(a)) of **13a**, **17a**, **22a**, and **33** had similar or greater negative charge compared to that of the corresponding imidazo[1,2-*b*]pyridazine **2**. These results suggested that scaffolds **A–D** might be promising hinge-binding templates because they could form tight hydrogen-bonding with the main chain of Cys919. Thus, to develop novel orally active type-II VEGFR2 kinase inhibitors, we designed and synthesized a series of imidazo[1,2-*a*]pyridine, [1,2,4]triazolo[1,5-*a*]pyridine, thiazolo[5,4-*b*]pyridine, and 1,3-benzothiazole derivatives.

2. Chemistry

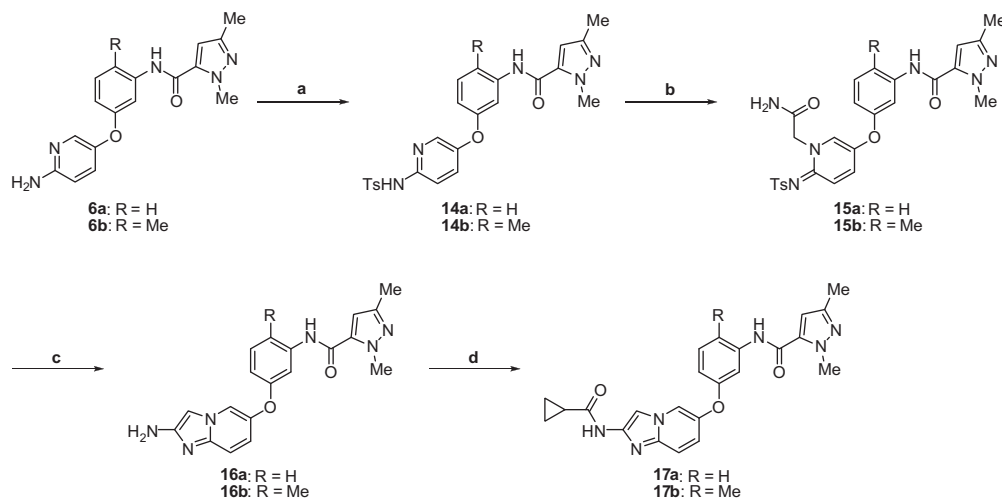
The general synthetic route for the preparation of [1,2,4]triazolo[1,5-*a*]pyridine derivatives is shown in Scheme 1. The coupling reaction of commercially available 3-nitrophenol (**3**) with 5-bromo-2-nitropyridine in the presence of cesium carbonate gave **4**, the nitro groups of which were converted to amino groups by hydrogenation to afford the diamine **5**. The selective acylation of **5** using acid chloride **8** furnished **6a** in 61% yield. Unfortunately, this route was limited to the synthesis of **6a** because the selective acylation of diamine analogues of **5** possessing an R sub-

stituent on the phenyl ring was generally unsuccessful. To obtain **6b–d**, therefore, the aminophenols **7a–c** were converted to the corresponding amides **9a–c** using **8**, followed by coupling with 5-bromo-2-nitropyridine and hydrogenation of **10a–c** with palladium–carbon (Pd/C) to afford desired compounds **6b–d**. Compounds **6a–d** were then converted to the corresponding thioureas **11a–d** using ethoxycarbonyl isothiocyanate, followed by treatment with hydroxylamine hydrochloride and *N,N*-diisopropylethylamine (DIEA) to give the 2-amino-[1,2,4]triazolo[1,5-*a*]pyridines **12a–d** in 63–75% yield. According to the literature,²⁶ we postulate that the 2-amino-[1,2,4]triazolo[1,5-*a*]pyridines **12a–d** were formed by oxadiazole formation of **11a–d** and subsequent rearrangement. Acylation of **12a,b** with cyclopropanecarbonyl chloride in the presence of triethylamine provided not only the desired amide derivatives **13a,b** but also the diacylated byproducts which had two cyclopropane carbonyl groups. Thus, the diacylated byproducts were converted to the monoacylated compounds **13a,b** by hydrolysis using aqueous sodium carbonate. On the other hand, acylation of **12c,d** with cyclopropanecarbonyl chloride in DMA without triethylamine provided only the desired monoacylated derivatives **13c,d** in 53% and 71% yield, respectively.

The preparation of imidazo[1,2-*a*]pyridine derivatives is shown in Scheme 2. Treatment of **6a,b** with *p*-toluenesulfonyl chloride



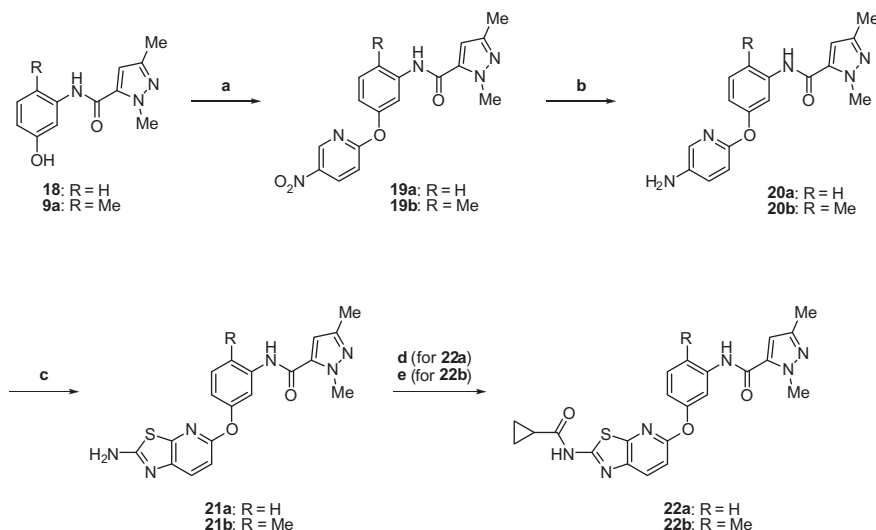
Scheme 1. Reagents and yields: (a) 5-Bromo-2-nitropyridine, Cs₂CO₃, DMF, 33%; (b) H₂, Pd/C, MeOH, 96%; (c) **8**, pyridine, THF, 61%; (d) Et₃N, THF, 63–99%; (e) 5-Bromo-2-nitropyridine, Cs₂CO₃, DMF, 44–59%; (f) H₂, Pd/C, MeOH, 88–95%; (g) EtOOCNCS, DMSO; (h) NH₂OH·HCl, DIEA, MeOH, EtOH, 63–75% for two steps; (i) (1) cyclopropanecarbonyl chloride, Et₃N, THF, (2) Na₂CO₃, MeOH, H₂O, 60% (**13a**), 60% (**13b**); (j) cyclopropanecarbonyl chloride, DMA, 53% (**13c**), 71% (**13d**).



Scheme 2. Reagents and yields: (a) TsCl, pyridine, 99% (**14a**) and 77% (**14b**); (b) iodoacetamide, DIEA, DMF, 71% (**15a**) and 72% (**15b**); (c) (1) TFAA, CH₂Cl₂ (2) NaOH, H₂O, EtOH; (d) cyclopropanecarbonyl chloride, Et₃N, THF, 21% (**17a**) and 41% (**17b**), for two steps.

gave **14a,b**, which were converted to **15a,b** using iodoacetamide. Formation of the imidazo[1,2-*a*]pyridine ring was achieved by the reaction of **15a,b** with trifluoroacetic anhydride (TFAA),²⁷ and subsequent hydrolysis to afford **16a,b**. Acylation of **16a,b** with cyclopropanecarbonyl chloride in the presence of triethylamine provided only the desired amide derivatives **17a,b**, respectively.

Thiazolo[5,4-*b*]pyridine derivatives were synthesized as illustrated in Scheme 3. Amide **18**, prepared from the reaction of 3-aminophenol with **8**, and compound **9a** were coupled with 2-chloro-5-nitropyridine in the presence of potassium carbonate to give **19a,b**. After hydrogenation of **19a,b** using Pd/C, the 3-aminopyridines **20a,b** were cyclized to the corresponding thiazolo[5,4-*b*]pyridines **21a,b** by treatment with bromine and potassium isothiocyanate in 51% and 47% yield, respectively.²⁸ Similar to the synthesis of **13a,b**, compound **22a** was synthesized by acylation of **21a** with cyclopropanecarbonyl chloride in the presence of triethylamine followed by hydrolysis of the diacylated byproduct with sodium carbonate. The selective monoacylation of **21b** was also accomplished by addition of cyclopropanecarbonyl chloride in DMA without any other base to give **22b** in 66% yield.



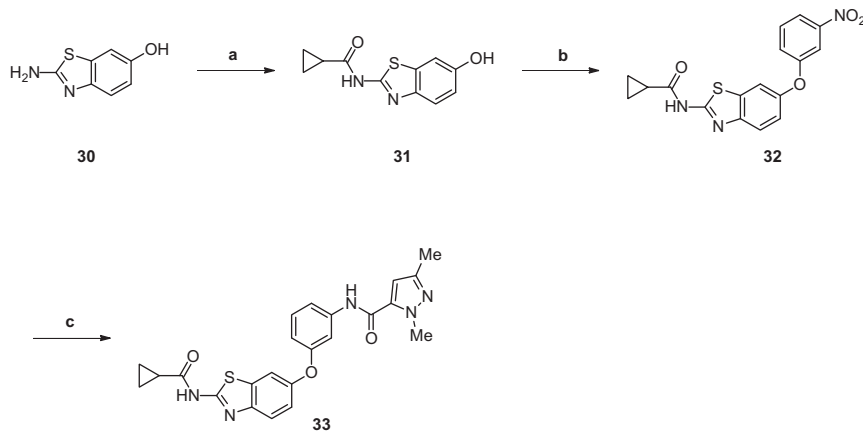
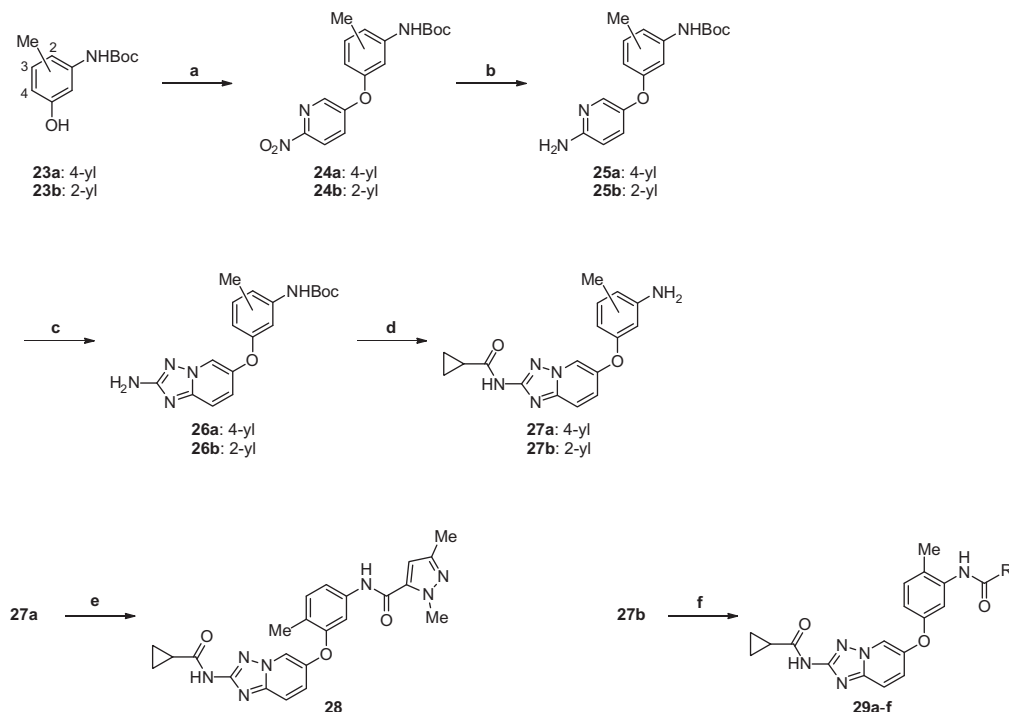
Scheme 3. Reagents and yields: (a) 2-Chloro-5-nitropyridine, K₂CO₃, DMF, 94% (**19a**) and 94% (**19b**); (b) H₂, Pd/C, MeOH, 86% (**20a**) and quant. (**20b**); (c) Br₂, KNCS, AcOH, 51% (**21a**) and 47% (**21b**); (d) (1) cyclopropanecarbonyl chloride, Et₃N, THF, (2) Na₂CO₃, MeOH, H₂O, 56%; (e) cyclopropanecarbonyl chloride, DMA, 66%.

[1,2,4]Triazolo[1,5-*a*]pyridine analogues were also synthesized as shown in Scheme 4. In a similar manner to the synthesis of **6b–d**, compounds **25a,b** were prepared by the coupling of **23a,b** with 5-bromo-2-nitropyridine and subsequent hydrogenation of the resulting nitro derivatives **24a,b**. Compounds **25a,b** were then cyclized to give the [1,2,4]triazolo[1,5-*a*]pyridines **26a** and **26b** in 87% and 49% yield, respectively. The 2-amino groups of **26a,b** were acylated followed by removal of the Boc protecting groups in acidic condition to give anilines **27a,b**. Acylation of **27a,b** with the corresponding acid chlorides furnished **28** and **29a–f** in 45–87% yield.

Scheme 5 depicts the synthesis of the 1,3-benzothiazole derivative **33**. Commercially available **30** was acylated with cyclopropanecarbonyl chloride to provide **31**, which was coupled with 1-fluoro-3-nitrobenzene to give nitro derivative **32**. Reduction of the nitro group of **32** and the subsequent acylation with acid chloride **8** afforded the desired product **33** in 5% yield.

3. Results and discussion

The compounds in Tables 1 and 3 were evaluated for their inhibitory activity against human VEGFR2 kinase in a non-RI assay

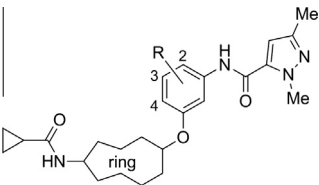


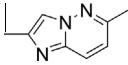
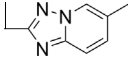

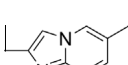
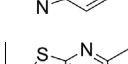
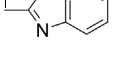
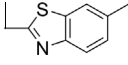
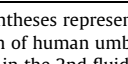
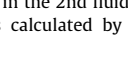

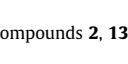
using the Alphascreen[®] system.²⁹ Compounds that showed potent VEGFR2 kinase inhibition were evaluated for their cellular activity in human umbilical vein endothelial cells (HUVEC).

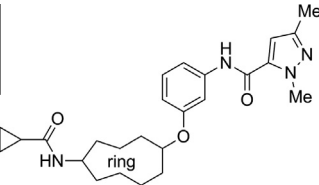
Table 1 summarizes the results of modifications to the hinge-binding core scaffold. Replacement of imidazo[1,2-*b*]pyridazine (**2**) with other 5,6-fused heterocycles possessing a nitrogen at the 1-position (**13a**, **17a**, **22a**, and **33**) retained strong VEGFR2 inhibitory activity. This result suggested that these compounds adopt similar binding modes to **2** with VEGFR2, with the N1-nitrogen forming a tight hydrogen bond with the NH group of Cys919. Moving the nitrogen of **2** from the 5-position to the 3-position (**13a**) as well as replacement of the N5-nitrogen of **2** with carbon (**17a**) did not affect VEGFR2 inhibition. These results suggest that there are no amino acid residues that could potentially hydrogen bond with these compounds in this region. In addition, the retention of po-

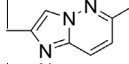
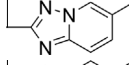
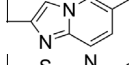
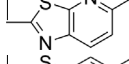
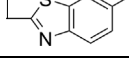
tency observed for **22a** and **33** revealed that the bridgehead nitrogen of **2** was not important for potency and the larger sulfur atom of **22a** and **33** did not perturb the hinge interactions. Compounds **13a**, **17a**, **22a**, and **33** also displayed similar cellular potency to **2** in the VEGF-driven HUVEC proliferation assay, revealing that [1,2,4]triazolo[1,5-*a*]pyridine, imidazo[1,2-*a*]pyridine, thiazolo[5,4-*b*]pyridine, and 1,3-benzothiazole are promising hinge-binding cores for VEGFR2 kinase inhibitors.

Table 2 shows the effect of the hinge-binding core on inhibitory activity against other kinases. Similar to the imidazo[1,2-*b*]pyridazine derivative **2**, compounds **13a**, **17a**, **22a** and **33** strongly inhibited VEGFR1 and PDGFR β kinase with IC₅₀ values of less than 100 nM. It has been reported that some type-II kinase inhibitors show inhibitory activity against not only the original target kinase but also other kinases which can adopt the DFG-out conforma-

Table 1Effect of modifications to the hinge-binding core^a


Compd	Ring	R	VEGFR2 IC ₅₀ (nM)	HUVEC ^b IC ₅₀ (nM)	Solubility JP2 ^c (μg/mL)	ClogP ^d
2		H	1.4 (1.3–1.5)	1.7 (0.66–3.8)	1.7	2.3
13a		H	1.1 (1.0–1.3)	3.9 (2.0–7.5)	1.2	2.4
13b		2-Me	1.9 (1.6–2.2)	1.3 (0.59–2.6)	53	2.2
13c		3-Me	2.1 (1.8–2.4)	47 (17–136)	3.2	2.9
28		4-Me	3.7 (3.3–4.3)	67 (48–92)	3.7	2.9
13d		2-F	2.0 (1.8–2.3)	5.0 (3.0–8.0)	65	1.9
17a		H	1.1 (1.0–1.2)	1.1 (0.34–2.6)	0.73	3.3
17b		2-Me	1.2 (1.1–1.3)	0.80 (0.38–1.5)	2.9	3.1
22a		H	1.3 (1.1–1.4)	4.4 (1.9–9.9)	<0.04	3.3
22b		2-Me	1.2 (1.0–1.4)	3.6 (1.4–8.6)	4.8	3.2
33		H	3.6 (3.0–4.3)	0.93 (0.12–3.7)	0.22	4.2

^a Numbers in parentheses represent 95% confidence interval.^b Growth inhibition of human umbilical vein endothelial cells (HUVEC).^c Kinetic solubility in the 2nd fluid of Disintegration Test of the Japanese Pharmacopoeia (pH 6.8).^d ClogP value was calculated by Daylight Software. ClogP, version 4.95, Daylight Software, Daylight chemical information systems, Inc., Aliso Viejo, CA; <http://www.daylight.com>.**Table 2**Kinase selectivity of compounds **2**, **13a**, **17a**, **22a**, and **33**^a


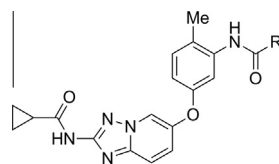
Compd	Ring	IC ₅₀ (nM) ^b							
		VEGFR1	VEGFR2	PDGFRβ	c-kit	Tie-2	Aurora A	B-raf	p38α
2		7.4 (6.4–8.4)	1.4 (1.3–1.5)	5.5 (3.8–7.9)	23 (19–27)	>1000	360 (240–530)	>1000	>1000
13a		33 (25–43)	1.1 (1.0–1.3)	19 (14–25)	130 (110–170)	>1000	120 (44–330)	290 (42–2000)	>1000
17a		6.4 (5.4–7.7)	1.1 (1.0–1.2)	5.9 (4.6–7.8)	21 (16–26)	>1000	170 (110–260)	>1000	>1000
22a		56 (36–87)	1.3 (1.1–1.4)	8.3 (4.6–15)	170 (110–260)	>1000	>1000	>1000	>1000
33		69 (62–77)	3.6 (3.0–4.3)	21 (14–33)	240 (190–290)	>1000	680 (150–3200)	>1000	>1000

^a Abbreviations of kinases are described in Section 5.^b Numbers in parentheses represent 95% confidence interval.

tion.²¹ For instance, a pyrrolo[3,2-*d*]pyrimidine-based VEGFR2 kinase inhibitor we previously reported has strong Tie-2 kinase inhibitory activity.²⁴ Thus, we investigated kinase selectivity against c-kit,³⁰ Aurora A,³¹ B-raf,³² Tie-2,³³ and p38 mitogen-acti-

vated protein kinase α (p38α)²² whose crystal structures with their type-II inhibitors have been reported. Interestingly, inhibitory activity against c-kit, Aurora A, and B-raf was different among these chemotypes, while Tie-2 and p38α were not strongly inhib-

Table 3
Modification of the acyl group^a



Compd	R	VEGFR2 IC ₅₀ (nM)	HUVEC ^b IC ₅₀ (nM)	Solubility JP2 ^c (μg/mL)	ClogP ^d
13b		1.9 (1.6–2.2)	1.3 (0.59–2.6)	53	2.2
29a		1.5 (1.3–1.7)	4.3 (1.5–12)	0.16	3.5
29b		0.48 (0.43–0.55)	1.6 (0.9–26)	1.2	3.7
29c		1.9 (1.7–2.2)	3.8 (1.5–9.3)	>93	1.9
29d		1.6 (1.4–1.7)	9.9 (4.3–23)	>80	1.9
29e		2.0 (1.7–2.2)	56 (33–96)	12	3.4
29f		3.0 (2.6–3.5)	88 (59–133)	>78	2.8

^a Numbers in parentheses represent 95% confidence interval.

^b Growth inhibition of human umbilical vein endothelial cells (HUVEC).

^c Kinetic solubility in the 2nd fluid of Disintegration Test of the Japanese Pharmacopoeia (pH 6.8).

^d ClogP value was calculated by Daylight Software. ClogP, version 4.95, Daylight Software, Daylight chemical information systems, Inc., Aliso Viejo, CA; <http://www.daylight.com>.

ited by any of the evaluated compounds even at a concentration of 1000 nM. Imidazo[1,2-*b*]pyridazine **2** and imidazo[1,2-*a*]pyridine **17a** inhibited c-kit more potently than the other three compounds, suggesting that the carbon atom at the 3-position of their bicyclic cores is favorable for c-kit inhibition. On the other hand, the fact that the [1,2,4]triazolo[1,5-*a*]pyridine **13a** showed the strongest inhibitory activity against B-raf kinase may suggest the importance of the nitrogen atom at the 3-position for B-raf inhibition. Unlike c-kit and B-raf, inhibition data for Aurora A showed less dependence on the hinge-binding core. Except for the thiazolo[5,4-*b*]pyridine **22a**, most of these compounds displayed moderate inhibition against Aurora A. These results revealed that modification of the hinge-binding core can be utilized to adjust kinase selectivity.

We next evaluated kinetic solubility for compounds in the neutral aqueous solution (JP2: the 2nd fluid of Disintegration Test of the Japanese Pharmacopoeia, pH 6.8). The measured solubility for

2 in JP2 was 1.7 μg/mL. Compared to **2**, compounds **13a** and **17a** showed similar solubility, while **22a** and **33** were found to be less soluble. The poor solubility of **22a** and **33** may be attributable to their higher lipophilicity.³⁴ Another hypothesis is that the intramolecular interaction between the S3-sulfur and the carbonyl oxygen at the 2-position might stabilize the planar conformations of **22a** and **33**, thus enabling tight crystal packing. Indeed, S···O interactions have been observed in a large number of organosulfur compounds controlling the conformation of small and large molecules.³⁵ On the other hand, introduction of a methyl group into the central benzene ring (**13b**, **17b**, **22b**) resulted in improvement of solubility, especially for the triazolo[1,5-*a*]pyridine **13b** (JP2 solubility: 53 μg/mL). The improved solubility brought by the methyl substituent might be due to distortion from molecular planarity and/or symmetry. Recently, Ishikawa et al. reported that disruption of molecular planarity leads to improvement of aqueous

Table 4
Pharmacokinetic properties of **2**, **13d**, and **29c**

Compd	Mouse PK ^a			Metabolic stability ^d		Solubility JP2 ^e (μg/mL)
	C _{max} (μg/mL)	AUC _{0–8h} ^b (μg·h/mL)	C _{8h} (μg/mL) ^c	Human (μL/min/mg)	Mouse (μL/min/mg)	
2	0.15	0.730	0.053	6.0	43	1.7
13d	3.11	7.39	0.247	10	45	65
29c	3.21	2.31	0.011	6.0	78	>93

^a Compounds were administered at an oral dose of 10 mg/kg as a cassette dosing.

^b Area under the plasma concentration–time curve.

^c Plasma concentration at 8 h after administration.

^d Metabolic stability in hepatic microsomes.

^e Kinetic solubility in the 2nd fluid of Disintegration Test of the Japanese Pharmacopoeia (pH 6.8).

solubility and lower melting points by decreased crystal packing energy.³⁶ In fact, the melting point (217–220 °C) of **13b** was lower than that of **13a** (244–245 °C).

Since **13b** exhibited not only strong inhibitory activity against VEGFR2 kinase but also improved solubility, we investigated more substitutions on the central benzene ring. Moving the methyl group of **13b** from the 2-position to the 3- or 4-position (**13c**, **28**) retained inhibitory activity against VEGFR2 kinase. On the other hand, **13c** and **28** were less potent than **13b** in HUVEC proliferation assay despite their retained enzyme activity, revealing that substitution at the 2-position was optimal. Further investigation revealed that substitution of the electron-withdrawing group at this position was also tolerated. In fact, the 2-fluoro derivative (**13d**) exhibited single-digit nanomolar IC₅₀ values in both of enzyme and cellular assays. As a result of kinetic solubility screening, **13d** (JP2 solubility: 65 µg/mL) showed improved solubility comparable to the 2-methyl derivative **13b**. One possible explanation for the improved solubility observed for **13d** could be due to its lower lipophilicity compared to **13a**.

The crystal structure of the complex between **2** and VEGFR2 (Fig. 2) indicated that modification of the terminal 1,3-dimethylpyrazole moiety would be possible because no pyrazole-specific interaction with the surrounding amino acid residues was observed. Thus, we examined the effect of the terminal acyl group (Table 3). As the co-crystal structure analysis suggested, a variety of acyl groups were tolerated with respect to enzymatic activity. Replacement of a pyrazole group (**13b**) with not only other heteroaromatic rings (**29a,b**) but also aliphatic groups (**29e,f**) retained strong VEGFR2 inhibitory activity. In contrast, cell activity and solubility showed a more marked dependence on the acyl group. As for HUVEC inhibition, the five-membered heterocycle derivatives (**29a–d**) were more potent than the aliphatic derivatives (**29e,f**). The fact that the compounds showing similar ClogP value (e.g. **29a** and **29e**) have different HUVEC inhibitory activity revealed that lipophilicity of compounds has little relation to their cellular activity. The planar structure of heteroaryl groups may rather contribute to enhance cellular activity. On the other hand, lipophilicity of compounds seemed to influence their solubility. For example, the monomethyl pyrazole derivative **29d** displayed improved solubility compared to the corresponding dimethyl pyrazole derivative **13b**. Similar tendency was observed in the dimethyl-substituted heteroaryl derivatives (**13b** and **29a,c**). Compared to **13b**, more polar **29c** showed improved solubility while less polar **29a** was much less soluble.

Compounds that displayed strong HUVEC inhibition and moderate solubility were selected for further evaluation (Table 4). Pharmacokinetic parameters for **2**, **13d**, and **29c** were measured in mice (cassette dosing). Compounds **13d** and **29c** showed higher

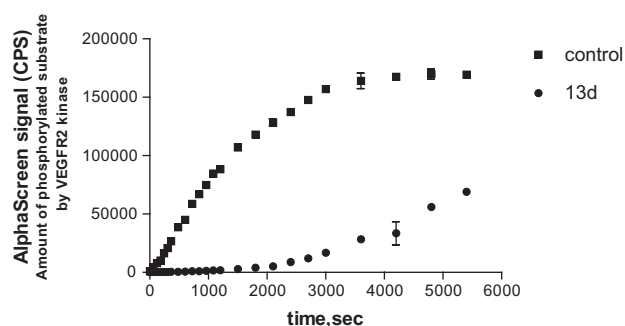


Figure 4. Dilution assay of VEGFR2–**13d** complex. Phosphorylation of peptide substrate as a function of time is shown. The reaction was initiated by diluting a preformed enzyme–inhibitor complex to one tenth of IC₅₀ with reaction buffer containing 1 mM ATP and 0.1 µg/mL biotinylated poly-Glu-Tyr (4:1). The recovery of activity was measured using the AlphaScreen® system.

Table 5
Preincubation time-dependent inhibition of **13d** and **29f**^a

Compd	VEGFR2 IC ₅₀ (nM) pre-incubation ^b		HUVEC ^c IC ₅₀ (nM)
	5 min	60 min	
13d	2.2 (2.0–2.5)	0.26 (0.25–0.28)	5.0 (3.0–8.0)
29f	3.9 (3.4–4.4)	3.1 (2.4–4.0)	88 (59–133)

^a Numbers in parentheses represent 95% confidence interval.

^b The assay was performed with preincubation of the compounds and VEGFR2 before addition of 1 mM of ATP.

^c Growth inhibition of human umbilical vein endothelial cells (HUVEC).

peak plasma concentrations (C_{max}) as well as area under the plasma concentration–time curve (AUC_{0–8h}) values than that of **2**, indicating that their improved solubilities might contribute to their improved pharmacokinetic properties. In particular, **13d** exhibited not only a favorable AUC value but also high plasma concentration at 8 h after administration (C_{8h}) reflecting its high stability in mouse hepatic microsomes. Since **13d** also showed high stability in human hepatic microsomes, it would be expected to have sufficient oral bioavailability in humans.

Recently, we demonstrated that pyrrolo[3,2-*d*]pyrimidine and imidazo[1,2-*b*]pyridazine derivatives inhibited VEGFR2 with very slow, reversible (pseudo-irreversible) kinetics.^{24,37,38} These favorable properties may contribute to their enhanced cell activity. Thus, we evaluated the VEGFR2 inhibition kinetics of the triazol[1,5-*a*]pyridine derivatives presented in this work. Table 5 shows the pre-incubation time dependency of compounds in VEGFR2 inhibition. Pre-incubation of **13d** and VEGFR2 for 60 min before addition of ATP to start the kinase reaction resulted in 10-fold enhancement of enzymatic activity (IC₅₀ = 0.26 nM) compared to that for 5 min of pre-incubation time (IC₅₀ = 2.2 nM). This time dependency indicated that **13d** possesses slow-binding kinetics against VEGFR2. On the other hand, **29f** did not show pre-incubation time dependency, suggesting that it is a fast-binding inhibitor. Inhibitory activity of the compounds with the longer preincubation was found to be better correlated with their HUVEC inhibitory activities. The VEGFR2 IC₅₀ value obtained with 60-min preincubation for compound **13d** was about 10-fold lower than that for **29f** (0.26 nM vs 3.1 nM), which supports the ratio of IC₅₀ values observed in the HUVEC proliferation assay (5.0 nM for **13d** vs 88 nM for **29f**). To better understand inhibition kinetics against VEGFR2 kinase, dilution assay of VEGFR2–**13d** complex was performed. When the pre-formed complex of **13d** and VEGFR2 was diluted to one tenth of IC₅₀ to dissociate the complex and the kinase reaction was initiated, the recovery of kinase activity was much slower than in the absence of compound (Fig. 4). The above results revealed that **13d** also possesses slow-dissociation kinetics. Advantages of compounds showing slow-dissociation kinetics include improvement of off-target selectivity and in vivo efficacy.³⁹ Thus,

Table 6
Kinase selectivity of **13d**^{a,b}

Kinase	IC ₅₀ (nM)	Kinase	IC ₅₀ (nM)
VEGFR2	2.0 (1.8–2.3)	IGF1-R	>10,000
VEGFR1	3.6 (3.3–3.8)	c-kit	150 (120–200)
PDGFRα	12 (10–14)	Src	>10,000
PDGFRβ	14 (11–17)	FAK	>10,000
FGFR1	2700 (1900–3900)	B-raf	>10,000
Tie-2	>10,000	ERK1	>10,000
HER2	>10,000	PKCθ	>10,000
EGFR	>10,000	GSK3β	>10,000
IR	>10,000	Aurora A	2900 (1800–4500)
p38α	>10,000		

^a Abbreviations of kinases are described in Section 5.

^b Numbers in parentheses represent 95% confidence interval.

Table 7
Antitumor efficacy of **13d** in nude mice bearing human tumor xenografts

Tumor model	Dose ^a (mg/kg)	T/C ^b (%)
DU145 (prostate)	0.5	60
	1.5	37
	5.0	27
A549 (NSCLC)	0.5	57
	1.5	34
	5.0	14

^a Compound was dosed twice daily for 14 days.

^b Treatment per control (T/C %), an index of antitumor efficacy, was calculated by comparison of the mean change in tumor volume over the treatment period for the control and treated groups.

13d is expected to show prolonged anti-tumor activity with fewer off-target effects in an in vivo setting.

We evaluated the kinase selectivity of compound **13d**, and the results are shown in Table 6. Compound **13d** was found to potentially inhibit platelet-derived growth factor receptor (PDGFR) family kinases in addition to the VEGFR kinases. Platelet-derived growth factor (PDGF) and the PDGFR signaling pathway are necessary for the pericyte recruitment during angiogenesis.⁴⁰ It was also suggested that inhibition of PDGF/PDGFR signaling is an effective way for blocking further tumor growth in end-stage tumors.⁴¹ Thus, simultaneous inhibition of VEGFR and PDGFR kinases may lead to synergistic effects in anti-angiogenic tumor therapy. The inhibitory potency of **13d** against several other protein kinases, such as human epidermal growth factor receptor 2 (HER2), epidermal growth factor receptor (EGFR), insulin receptor (IR), and protein kinase C θ (PKC θ) were all over 1000 nM, with c-kit showing the most potent off-target inhibition (IC₅₀ = 150 nM). These results revealed that **13d** is a highly selective and potent inhibitor of VEGFR/PDGFR kinases.

Finally, we evaluated the antitumor efficacy of **13d** in DU145 (human prostate cancer) and A549 (non-small cell lung cancer) xenograft models in nude mice (Table 7). Consistent with its potent cellular activity and good oral exposure profiles, **13d** showed significant anti-tumor efficacy in the both models tested when dosed orally at 10 mg/kg daily (5.0 mg/kg, bid). Under these conditions, neither body weight loss nor obvious signs of toxicity were observed (data not shown).

4. Conclusion

By replacement of the imidazo[1,2-*b*]pyridazine core of **2** with [1,2,4]triazolo[1,5-*a*]pyridine (**13a**), the imidazo[1,2-*a*]pyridine (**17a**), the thiazolo[5,4-*b*]pyridine (**22a**), and 1,3-benzothiazole (**33**), we developed a novel series of type-II VEGFR2 kinase inhibitors. Further optimization revealed that introduction of a substituent into the central benzene ring of the [1,2,4]triazolo[1,5-*a*]pyridine **13a** and subsequent modification of the terminal pyrazole moiety (**13d** and **29c**) led to improvement of solubility, which resulted in improved pharmacokinetic properties. Results of further studies revealed that representative compound **13d** inhibited VEGFR2 kinase with slow dissociation kinetics and showed strong inhibitory activity against PDGFR kinases. Consistent with its favorable profile described above, **13d** showed potent antitumor efficacy without obvious signs of toxicity in DU145 and A549 mouse xenograft models. Thus, based on its slow dissociation kinetics and potent VEGFR/PDGFR kinase inhibitory activities, compound **13d** shows great promise as an anticancer agent.

5. Experimental

Melting points were determined on a BÜCHI Melting Point B-545, and were not corrected. Proton nuclear magnetic resonance (¹H NMR) spectra were recorded on Varian Mercury 300

(300 MHz) or Bruker DPX300 (300 MHz) instruments. Chemical shifts are reported as δ values (ppm) downfield from internal tetramethylsilane of the indicated organic solution. Peak multiplicities are expressed as follows: s, singlet; d, doublet; t, triplet; q, quartet; dd, doublet of doublet; ddd, doublet of doublet of doublets; dt, doublet of triplet; br s, broad singlet; m, multiplet. Coupling constants (*J* values) are given in hertz (Hz). Elemental analyses were carried out by Takeda Analytical Laboratories. Reaction progress was determined by thin layer chromatography (TLC) analysis on silica gel 60 F254 plate (Merck) or NH TLC plates (Fuji Silysia chemical Ltd.). Chromatographic purification was carried on silica gel columns 60 (0.063–0.200 mm or 0.040–0.063 mm, Merck), basic silica gel (ChromatorexNH, 100–200 mesh, Fuji silysia chemical Ltd) or Purif-Pack (SI 60 IM or NH 60 IM, Fuji Silysia, Ltd). Commercial reagents and solvents were used without additional purification. Abbreviations are used as follows: CDCl₃, deuterated chloroform; DMSO-*d*₆, dimethyl sulfoxide-*d*₆; AcOEt, ethyl acetate; DMF, *N,N*-dimethylformamide; MeOH, methanol; THF, tetrahydrofuran; EtOH, ethanol; DMSO, dimethyl sulfoxide; DMA, *N,N*-dimethylacetamide.

5.1. 2-Nitro-5-(3-nitrophenoxy)pyridine (**4**)

A mixture of **3** (7.76 g, 55.8 mmol), 5-bromo-2-nitropyridine (10.3 g, 50.7 mmol), cesium carbonate (24.8 g, 76.1 mmol), and DMF (150 mL) was stirred at 50 °C for 15 h. The mixture was diluted with water and extracted with AcOEt. The extract was washed with water and brine, dried over anhydrous magnesium sulfate, and concentrated under reduced pressure. The residue was purified by basic silica gel column chromatography (AcOEt/hexane) to give **4** (4.37 g, 33%) as a yellow solid: ¹H NMR (DMSO-*d*₆) δ 7.73–7.85 (3H, m), 8.10 (1H, t, *J* = 2.1 Hz), 8.15–8.19 (1H, m), 8.38 (1H, dd, *J* = 9.0, 0.6 Hz), 8.52–8.54 (1H, m).

5.2. 5-(3-Aminophenoxy)pyridin-2-amine (**5**)

A mixture of **4** (1.33 g, 5.07 mmol), 10% palladium on carbon (water ~50%, 100 mg), and MeOH (10 mL) was stirred under a hydrogen atmosphere at room temperature for 12 h. The catalyst was filtered off, and the filtrate was concentrated in vacuo to give **5** (980 mg, 96%) as a yellow oil: ¹H NMR (DMSO-*d*₆) δ 5.15 (2H, br s), 5.82 (2H, br s), 6.00–6.04 (2H, m), 6.18–6.22 (1H, m), 6.47 (1H, d, *J* = 8.9 Hz), 6.90 (1H, t, *J* = 7.7 Hz), 7.14 (1H, dd, *J* = 8.9, 3.0 Hz), 7.69 (1H, d, *J* = 3.0 Hz).

5.3. *N*-{3-[(6-Aminopyridin-3-yl)oxy]phenyl}-1,3-dimethyl-1*H*-pyrazole-5-carboxamide (**6a**)

To a solution of **5** (975 mg, 4.85 mmol), pyridine (410 μ L, 5.09 mmol) in THF (10 mL) was added a solution of **8** (807 mg, 5.09 mmol) in THF (10 mL) dropwise at 0 °C, and the mixture was stirred at room temperature for 2 h. The mixture was diluted with water and extracted with AcOEt. The extract was washed with brine, dried over anhydrous magnesium sulfate, and concentrated under reduced pressure. The residue was purified by silica gel column chromatography (AcOEt/hexane) followed by recrystallization from AcOEt–hexane to give **6a** (964 mg, 61%) as a white solid: ¹H NMR (DMSO-*d*₆) δ 2.18 (3H, s), 3.96 (3H, s), 5.91 (2H, br s), 6.50 (1H, d, *J* = 8.9 Hz), 6.65–6.68 (1H, m), 6.78 (1H, s), 7.11 (1H, dd, *J* = 8.9, 3.0 Hz), 7.24–7.30 (2H, m), 7.43–7.47 (1H, m), 7.75 (1H, d, *J* = 3.0 Hz), 10.10 (1H, br s).

5.4. *N*-{5-[(6-Aminopyridin-3-yl)oxy]-2-methylphenyl}-1,3-dimethyl-1*H*-pyrazole-5-carboxamide (**6b**)

A mixture of **10a** (3.38 g, 9.20 mmol), 10% palladium on carbon (water ~50%, 300 mg), and MeOH (20 mL) was stirred under a

hydrogen atmosphere at room temperature for 4 h. The catalyst was filtered off, and the filtrate was concentrated in vacuo to give **6b** (2.94 g, 95%) as a white solid: ^1H NMR (DMSO- d_6) δ 2.15 (3H, s), 2.18 (3H, s), 3.97 (3H, s), 5.88 (2H, br s), 6.49 (1H, dd, J = 9.0, 0.6 Hz), 6.73–6.78 (2H, m), 6.88 (1H, d, J = 2.4 Hz), 7.17–7.22 (2H, m), 7.73–7.75 (1H, m), 9.71 (1H, br s).

5.5. *N*-{3-[(6-Aminopyridin-3-yl)oxy]-5-methylphenyl}-1,3-dimethyl-1*H*-pyrazole-5-carboxamide (**6c**)

The compound **6c** was prepared from **10b** in a manner similar to that described for **6b** to yield a pale yellow oil (88%): ^1H NMR (CDCl₃) δ 2.28 (3H, s), 2.31 (3H, s), 4.12 (3H, s), 4.40 (2H, s), 6.40 (1H, s), 6.50–6.57 (2H, m), 6.92 (1H, t, J = 2.0 Hz), 7.17 (1H, s), 7.21 (1H, dd, J = 8.6, 2.6 Hz), 7.65 (1H, s), 7.89–7.92 (1H, m).

5.6. *N*-{5-[(6-Aminopyridin-3-yl)oxy]-2-fluorophenyl}-1,3-dimethyl-1*H*-pyrazole-5-carboxamide (**6d**)

The compound **6d** was prepared from **10c** in a manner similar to that described for **6b** to yield a white solid (88%): ^1H NMR (DMSO- d_6) δ 2.18 (3H, s), 3.96 (3H, s), 5.90 (2H, s), 6.50 (1H, d, J = 9.0 Hz), 6.76–6.85 (2H, m), 7.10 (1H, dd, J = 6.2, 3.2 Hz), 7.16–7.28 (2H, m), 7.76 (1H, d, J = 3.0 Hz), 9.97 (1H, s).

5.7. *N*-(5-Hydroxy-2-methylphenyl)-1,3-dimethyl-1*H*-pyrazole-5-carboxamide (**9a**)

To a solution of **7a** (3.71 g, 30.1 mmol), triethylamine (4.38 mL, 31.6 mmol) in THF (30 mL) was added a solution of **8** (5.02 g, 31.6 mmol) in THF (10 mL) dropwise at 0 °C, and the mixture was stirred at room temperature for 15 h. The mixture was diluted with water and extracted with AcOEt. The extract was washed with brine, dried over anhydrous magnesium sulfate, and concentrated under reduced pressure. The residue was collected by filtration and washed with AcOEt–hexane to give **9a** (4.67 g, 63%) as a white solid: ^1H NMR (DMSO- d_6) δ 2.09 (3H, s), 2.19 (3H, s), 3.98 (3H, s), 6.57 (1H, dd, J = 8.5, 2.4 Hz), 6.76–6.79 (2H, m), 7.02 (1H, d, J = 8.5 Hz), 9.26 (1H, br s), 9.59 (1H, s).

5.8. *N*-(3-Hydroxy-5-methylphenyl)-1,3-dimethyl-1*H*-pyrazole-5-carboxamide (**9b**)

The compound **9b** was prepared from **7b** and **8** in a manner similar to that described for **9a** to yield a pale yellow oil (96%): ^1H NMR (CDCl₃) δ 2.29 (3H, s), 2.30 (3H, s), 4.13 (3H, s), 5.58 (1H, s), 6.39 (1H, s), 6.49 (1H, s), 6.80 (1H, s), 7.13 (1H, t, J = 2.0 Hz), 7.55 (1H, s).

5.9. *N*-(2-Fluoro-5-hydroxyphenyl)-1,3-dimethyl-1*H*-pyrazole-5-carboxamide (**9c**)

The compound **9c** was prepared from **7c** and **8** in a manner similar to that described for **9a** to yield a white solid (99%): ^1H NMR (DMSO- d_6) δ 2.19 (3H, s), 3.98 (3H, s), 6.58–6.64 (1H, m), 6.83 (1H, s), 6.97–7.09 (2H, m), 9.87 (1H, s), 1H not detected.

5.10. 1,3-Dimethyl-*N*-{2-methyl-5-[(6-nitropyridin-3-yl)oxy]phenyl}-1*H*-pyrazole-5-carboxamide (**10a**)

A mixture of **9a** (4.67 g, 19.0 mmol), 5-bromo-2-nitropyridine (3.68 g, 18.1 mmol), cesium carbonate (9.29 g, 28.5 mmol), and DMF (20 mL) was stirred at room temperature for 15 h. The mixture was diluted with water and extracted with AcOEt. The extract was washed with water and brine, dried over anhydrous magnesium sulfate, and concentrated under reduced pressure. The resi-

due was purified by silica gel column chromatography (AcOEt/hexane) and basic silica gel column chromatography (AcOEt/hexane) to give **10a** (3.38 g, 44%) as a white solid: ^1H NMR (DMSO- d_6) δ 2.20 (3H, s), 2.27 (3H, s), 3.98 (3H, s), 6.82 (1H, s), 7.09 (1H, dd, J = 8.3, 2.5 Hz), 7.31 (1H, d, J = 2.5 Hz), 7.41 (1H, d, J = 8.3 Hz), 7.62 (1H, dd, J = 8.8, 2.8 Hz), 8.36 (1H, d, J = 8.8 Hz), 8.42 (1H, d, J = 2.8 Hz), 9.82 (1H, s).

5.11. 1,3-Dimethyl-*N*-{3-methyl-5-[(6-nitropyridin-3-yl)oxy]phenyl}-1*H*-pyrazole-5-carboxamide (**10b**)

The compound **10b** was prepared from **9b** in a manner similar to that described for **10a** to yield a pale yellow oil (54%): ^1H NMR (CDCl₃) δ 2.29 (3H, s), 2.39 (3H, s), 4.12 (3H, s), 6.73 (1H, s), 7.19 (1H, s), 7.43 (1H, t, J = 2.0 Hz), 7.46 (1H, dd, J = 8.8, 3.0 Hz), 7.74 (1H, s), 8.01 (1H, s), 8.25 (1H, d, J = 8.8 Hz), 8.34 (1H, d, J = 3.0 Hz).

5.12. *N*-{2-Fluoro-5-[(6-nitropyridin-3-yl)oxy]phenyl}-1,3-dimethyl-1*H*-pyrazole-5-carboxamide (**10c**)

The compound **10c** was prepared from **9c** in a manner similar to that described for **10a** to yield a white solid (59%): ^1H NMR (DMSO- d_6) δ 2.20 (3H, s), 3.99 (3H, s), 6.87 (1H, s), 7.16–7.22 (1H, m), 7.46 (1H, dd, J = 10.5, 8.9 Hz), 7.59 (1H, dd, J = 6.3, 3.0 Hz), 7.66 (1H, dd, J = 9.5, 2.9 Hz), 8.36 (1H, d, J = 9.3 Hz), 8.44 (1H, d, J = 2.7 Hz), 1H not detected.

5.13. *N*-{3-[(2-Amino[1,2,4]triazolo[1,5-*a*]pyridin-6-yl)oxy]phenyl}-1,3-dimethyl-1*H*-pyrazole-5-carboxamide (**12a**)

To a solution of **6a** (184 mg, 0.569 mmol) in DMSO (4 mL) was added ethoxycarbonyl isothiocyanate (89.6 mg, 0.682 mmol), and the mixture was stirred at room temperature for 15 h. The mixture was diluted with water and extracted with AcOEt. The extract was washed with brine, dried over anhydrous magnesium sulfate, and concentrated under reduced pressure to give **11a** (268 mg, 99%) as a colorless oil. A mixture of **11a** (238 mg, 0.524 mmol), hydroxylammonium chloride (364 mg, 5.24 mmol), *N,N*-diisopropylethylamine (548 μL , 3.14 mmol), EtOH (3 mL), and MeOH (3 mL) was stirred at 60 °C for 5 h and 80 °C for 2 h. The mixture was diluted with water and extracted with AcOEt. The extract was washed with water and brine, dried over anhydrous magnesium sulfate, and concentrated under reduced pressure. The residue was purified by silica gel column chromatography (AcOEt/hexane and AcOEt/MeOH) and recrystallized from AcOEt–hexane to give **12a** (131 mg, 69%) as a white solid: ^1H NMR (DMSO- d_6) δ 2.18 (3H, s), 3.96 (3H, s), 6.03 (2H, s), 6.78–6.82 (2H, m), 7.30–7.43 (4H, m), 7.52–7.57 (1H, m), 8.65 (1H, d, J = 2.4 Hz), 10.13 (1H, s).

5.14. *N*-{5-[(2-Amino[1,2,4]triazolo[1,5-*a*]pyridin-6-yl)oxy]-2-methylphenyl}-1,3-dimethyl-1*H*-pyrazole-5-carboxamide (**12b**)

The compound **12b** was prepared from **6b** in a manner similar to that described for **12a** to yield a white solid (75%): ^1H NMR (DMSO- d_6) δ 2.18 (6H, s), 3.96 (3H, s), 5.99 (2H, s), 6.77 (1H, s), 6.87 (1H, dd, J = 8.6, 2.6 Hz), 7.02 (1H, d, J = 2.6 Hz), 7.23–7.29 (2H, m), 7.38 (1H, d, J = 9.3 Hz), 8.55 (1H, d, J = 1.8 Hz), 9.73 (1H, s).

5.15. *N*-{3-[(2-Amino[1,2,4]triazolo[1,5-*a*]pyridin-6-yl)oxy]-5-methylphenyl}-1,3-dimethyl-1*H*-pyrazole-5-carboxamide (**12c**)

The compound **12c** was prepared from **6c** in a manner similar to that described for **12a** to yield a white solid (63%): ^1H NMR (DMSO- d_6) δ 2.17 (3H, s), 2.28 (3H, s), 3.96 (3H, s), 6.01 (2H, s), 6.63 (1H, s), 6.77 (1H, s), 7.17 (1H, t, J = 1.9 Hz), 7.25–7.34 (1H, m), 7.36–7.45 (2H, m), 8.61 (1H, d, J = 1.9 Hz), 10.03 (1H, s).

5.16. N-[5-[(2-Amino[1,2,4]triazolo[1,5-*a*]pyridin-6-yl)oxy]-2-fluorophenyl]-1,3-dimethyl-1*H*-pyrazole-5-carboxamide (12d)

The compound **12d** was prepared from **6d** in a manner similar to that described for **12a** to yield a yellow solid (69%): ¹H NMR (DMSO-*d*₆) δ 2.18 (3H, s), 3.96 (3H, s), 6.02 (2H, s), 6.82 (1H, s), 6.92–6.98 (1H, m), 7.23–7.33 (3H, m), 7.40 (1H, dd, *J* = 9.3, 0.6 Hz), 8.61 (1H, dd, *J* = 2.1, 0.6 Hz), 10.01 (1H, s).

5.17. N-[3-[(2-[(Cyclopropylcarbonyl)amino][1,2,4]triazolo[1,5-*a*]pyridin-6-yl)oxy]phenyl]-1,3-dimethyl-1*H*-pyrazole-5-carboxamide (13a)

To a solution of **12a** (117 mg, 0.322 mmol), triethylamine (134 μL, 0.966 mmol) in THF (5 mL) was added cyclopropanecarbonyl chloride (38.0 μL, 0.419 mmol) at 0 °C, and the mixture was stirred at room temperature for 12 h. Cyclopropanecarbonyl chloride (29.3 μL, 0.322 mmol) was added to the mixture, and the resulting mixture was stirred at room temperature for 3 h. The mixture was diluted with water and extracted with AcOEt. The extract was washed with water and brine, dried over anhydrous magnesium sulfate, and concentrated under reduced pressure. To the residue thus obtained was added Na₂CO₃ (100 mg), MeOH (2 mL), and water (100 μL). The mixture was stirred at 50 °C for 30 min. The mixture was diluted with water and extracted with AcOEt. The extract was washed with water and brine, dried over anhydrous magnesium sulfate, and concentrated under reduced pressure. The residue was purified by silica gel column chromatography (AcOEt) followed by recrystallization from AcOEt to give **13a** (112 mg, 60%) as white crystals: mp 244–245 °C; ¹H NMR (DMSO-*d*₆) δ 0.80–0.85 (4H, m), 2.00–2.01 (1H, m), 2.17 (3H, s), 3.96 (3H, s), 6.77–6.85 (2H, m), 7.35 (1H, t, *J* = 8.3 Hz), 7.40 (1H, t, *J* = 2.1 Hz), 7.51–7.58 (2H, m), 7.74 (1H, d, *J* = 9.3 Hz), 8.94 (1H, d, *J* = 2.4 Hz), 10.14 (1H, s), 11.05 (1H, s); Anal. Calcd for C₂₂H₂₁N₇O₃·0.25AcOEt: C, 60.92; H, 5.11; N, 21.62. Found: C, 61.10; H, 5.21; N, 21.38.

5.18. N-[5-[(2-[(Cyclopropylcarbonyl)amino][1,2,4]triazolo[1,5-*a*]pyridin-6-yl)oxy]-2-methylphenyl]-1,3-dimethyl-1*H*-pyrazole-5-carboxamide (13b)

The compound **13b** was prepared from **12b** in a manner similar to that described for **13a** to yield white crystals (60%): mp 217–220 °C; ¹H NMR (DMSO-*d*₆) δ 0.81–0.83 (4H, m), 1.98–2.10 (1H, m), 2.18 (3H, s), 2.19 (3H, s), 3.96 (3H, s), 6.78 (1H, s), 6.92 (1H, dd, *J* = 8.4, 2.6 Hz), 7.07 (1H, d, *J* = 2.6 Hz), 7.27 (1H, d, *J* = 8.4 Hz), 7.49 (1H, dd, *J* = 9.5, 2.3 Hz), 7.71 (1H, d, *J* = 9.5 Hz), 8.53 (1H, d, *J* = 2.3 Hz), 9.76 (1H, s), 11.04 (1H, s); Anal. Calcd for C₂₃H₂₃N₇O₃·0.25EtOAc: C, 61.66; H, 5.39; N, 20.97. Found: C, 61.28; H, 5.36; N, 20.95.

5.19. N-[3-[(2-[(Cyclopropylcarbonyl)amino][1,2,4]triazolo[1,5-*a*]pyridin-6-yl)oxy]-5-methylphenyl]-1,3-dimethyl-1*H*-pyrazole-5-carboxamide (13c)

To a solution of **12c** (303 mg, 0.803 mmol) in DMA (10 mL) was added cyclopropanecarbonyl chloride (74.0 μL, 0.815 mmol) dropwise at 0 °C, and the mixture was stirred at room temperature for 15 h. The mixture was diluted with water and extracted with AcOEt. The extract was washed with brine, dried over anhydrous magnesium sulfate, and concentrated under reduced pressure. The residual solid was crystallized from AcOEt–hexane to give **13c** (188 mg, 53%) as white crystals: mp 233 °C; ¹H NMR (DMSO-*d*₆) δ 0.77–0.87 (4H, m), 1.96–2.10 (1H, m), 2.17 (3H, s), 2.29 (3H, s), 3.96 (3H, s), 6.67 (1H, s), 6.78 (1H, s), 7.21 (1H, t, *J* = 1.9 Hz), 7.43 (1H, s), 7.52 (1H, dd, *J* = 9.6, 2.3 Hz), 7.74 (1H, d, *J* = 9.6 Hz),

8.91 (1H, d, *J* = 2.3 Hz), 10.05 (1H, s), 11.04 (1H, s); Anal. Calcd for C₂₃H₂₃N₇O₃: C, 62.01; H, 5.20; N, 22.01. Found: C, 62.00; H, 5.22; N, 22.10.

5.20. N-[5-[(2-[(Cyclopropylcarbonyl)amino][1,2,4]triazolo[1,5-*a*]pyridin-6-yl)oxy]-2-fluorophenyl]-1,3-dimethyl-1*H*-pyrazole-5-carboxamide (13d)

The compound **13d** was prepared from **12d** in a manner similar to that described for **13c** to yield white crystals (71%); mp 209 °C; ¹H NMR (DMSO-*d*₆) δ 0.81–0.84 (4H, m), 1.99–2.08 (1H, m), 2.18 (3H, s), 3.96 (3H, s), 6.81 (1H, s), 6.98–7.03 (1H, m), 7.29–7.35 (2H, m), 7.52 (1H, dd, *J* = 9.6, 2.4 Hz), 7.73 (1H, d, *J* = 9.6 Hz), 8.87 (1H, d, *J* = 2.4 Hz), 10.02 (1H, s), 11.02 (1H, s); Anal. Calcd for C₂₂H₂₀FN₇O₃: C, 58.79; H, 4.49; N, 21.82. Found: C, 58.61; H, 4.36; N, 21.65.

5.21. 1,3-Dimethyl-N-[3-[(6-[(4-methylphenyl)sulfonyl]amino)pyridin-3-yl]oxy]phenyl]-1*H*-pyrazole-5-carboxamide (14a)

A mixture of **6a** (750 mg, 2.32 mmol), *para*-toluenesulfonyl chloride (486 mg, 2.55 mmol), and pyridine (6 mL) was stirred at 80 °C for 15 h. The mixture was diluted with water and extracted with AcOEt. The extract was washed with brine, dried over anhydrous magnesium sulfate, and concentrated under reduced pressure to give **14a** (1.13 g, 99%) as a colorless oil: ¹H NMR (DMSO-*d*₆) δ 2.18 (3H, s), 2.35 (3H, s), 3.33 (3H, s), 6.71–6.77 (2H, s), 7.13 (1H, d, *J* = 8.7 Hz), 7.29–7.53 (6H, m), 7.78 (2H, d, *J* = 8.4 Hz), 8.01 (1H, d, *J* = 3.0 Hz), 10.14 (1H, s), 11.06 (1H, br s).

5.22. 1,3-Dimethyl-N-[2-methyl-5-[(6-[(4-methylphenyl)sulfonyl]amino)pyridin-3-yl]oxy]phenyl]-1*H*-pyrazole-5-carboxamide (14b)

The compound **14b** was prepared from **6b** in a manner similar to that described for **14a** to yield a white solid (77%): ¹H NMR (DMSO-*d*₆) δ 2.19 (6H, s), 2.34 (3H, s), 3.97 (3H, s), 6.78–6.84 (2H, m), 6.98 (1H, d, *J* = 2.7 Hz), 7.13 (1H, d, *J* = 8.9 Hz), 7.25 (1H, d, *J* = 8.7 Hz), 7.36 (2H, d, *J* = 8.1 Hz), 7.44 (1H, dd, *J* = 8.9, 3.0 Hz), 7.77 (2H, d, *J* = 8.1 Hz), 7.97 (1H, d, *J* = 3.0 Hz), 9.73 (1H, s), 11.02 (1H, br s).

5.23. N-[3-[[1-(2-Amino-2-oxoethyl)-6-[(4-methylphenyl)sulfonyl]imino]-1,6-dihydropyridin-3-yl]oxy]phenyl]-1,3-dimethyl-1*H*-pyrazole-5-carboxamide (15a)

A mixture of **14a** (1.11 g, 2.32 mmol), *N,N*-diisopropylethylamine (424 μL, 2.44 mmol), and DMF (7 mL) was stirred at room temperature for 2 h. Iodoacetamide (451 mg, 2.44 mmol) was added to the mixture, and the resulting mixture was stirred at room temperature for 15 h. The mixture was diluted with water and extracted with AcOEt. The extract was washed with brine, dried over anhydrous magnesium sulfate, and concentrated under reduced pressure. The residue was collected by filtration and washed with AcOEt–hexane to give **15a** (883 mg, 71%) as a white solid: ¹H NMR (DMSO-*d*₆) δ 2.19 (3H, s), 2.34 (3H, s), 3.97 (3H, s), 4.83 (2H, s), 6.72–6.79 (2H, m), 7.26–7.43 (6H, m), 7.52–7.56 (1H, m), 7.66–7.77 (4H, m), 8.12 (1H, d, *J* = 2.7 Hz), 10.18 (1H, s).

5.24. N-[5-[[1-(2-Amino-2-oxoethyl)-6-[(4-methylphenyl)sulfonyl]imino]-1,6-dihydropyridin-3-yl]oxy]-2-methylphenyl]-1,3-dimethyl-1*H*-pyrazole-5-carboxamide (15b)

The compound **15b** was prepared from **14b** in a manner similar to that described for **15a** to yield a white solid (72%): ¹H

NMR (DMSO- d_6) δ 2.17 (3H, s), 2.19 (3H, s), 2.34 (3H, s), 3.98 (3H, s), 4.82 (2H, s), 6.79 (1H, s), 6.84 (1H, dd, J = 8.3, 2.6 Hz), 7.04 (1H, d, J = 2.6 Hz), 7.24–7.29 (3H, m), 7.37–7.42 (2H, m), 7.65–7.71 (3H, m), 7.76 (1H, br s), 8.10 (1H, d, J = 3.0 Hz), 9.77 (1H, s).

5.25. *N*-{3-[(2-Aminoimidazo[1,2-*a*]pyridin-6-yl)oxy]phenyl}-1,3-dimethyl-1*H*-pyrazole-5-carboxamide (16a)

A mixture of **15a** (882 mg, 1.65 mmol), trifluoroacetic anhydride (6 mL), and dichloromethane (8 mL) was stirred at room temperature for 2.5 h. The mixture was concentrated under reduced pressure and the residue was partitioned with AcOEt and saturated aqueous sodium hydrogen carbonate. The organic layer was separated and washed with brine, dried over anhydrous magnesium sulfate, and concentrated under reduced pressure. The residue was purified by silica gel column chromatography (AcOEt/hexane) to give 1,3-dimethyl-*N*-{3-[(trifluoroacetyl)amino]imidazo[1,2-*a*]pyridin-6-yl)oxy]phenyl}-1*H*-pyrazole-5-carboxamide (338 mg, 45%) as a white solid. The solid thus obtained (328 mg, 0.715 mmol) was dissolved in 1 N NaOH (3 mL), EtOH (3 mL), and the solution was stirred at 40 °C for 2 h. The mixture was diluted with water and extracted with AcOEt. The extract was washed with brine, dried over anhydrous magnesium sulfate, and concentrated under reduced pressure. The residue was purified by silica gel column chromatography (AcOEt/MeOH) to give **16a** (205 mg, 79%) as a white solid: ^1H NMR (DMSO- d_6) δ 2.17 (3H, s), 3.96 (3H, s), 5.09 (2H, s), 6.75–6.78 (2H, m), 6.86 (1H, dd, J = 9.4, 2.0 Hz), 7.01 (1H, s), 7.22 (1H, d, J = 9.4 Hz), 7.32 (1H, d, J = 8.3 Hz), 7.37 (1H, t, J = 2.3 Hz), 7.50–7.60 (1H, m), 8.33 (1H, d, J = 2.0 Hz), 10.12 (1H, s).

5.26. *N*-{3-[(2-[(Cyclopropylcarbonyl)amino]imidazo[1,2-*a*]pyridin-6-yl)oxy]phenyl}-1,3-dimethyl-1*H*-pyrazole-5-carboxamide (17a)

To a solution of **16a** (270 mg, 0.745 mmol), triethylamine (310 μL , 2.24 mmol) in THF (5 mL) was added a solution of cyclopropanecarbonyl chloride (88.0 μL , 0.969 mmol) at 0 °C, and the mixture was stirred at room temperature for 15 h. The mixture was diluted with water and extracted with AcOEt. The extract was washed with water and brine, dried over anhydrous magnesium sulfate, and concentrated under reduced pressure. The residue was purified by silica gel column chromatography (AcOEt/hexane) followed by recrystallization from AcOEt–hexane to give **17a** (191 mg, 60%) as white crystals: mp 226–230 °C; ^1H NMR (DMSO- d_6) δ 0.79–0.81 (4H, m), 1.89–1.97 (1H, m), 2.17 (3H, s), 3.95 (3H, s), 6.77–6.81 (2H, m), 7.08 (1H, dd, J = 9.8, 2.4 Hz), 7.33 (1H, t, J = 8.3 Hz), 7.39 (1H, t, J = 2.1 Hz), 7.46–7.56 (2H, m), 8.06 (1H, s), 8.58 (1H, d, J = 2.4 Hz), 10.12 (1H, s), 10.97 (1H, s); Anal. Calcd for $\text{C}_{23}\text{H}_{22}\text{N}_6\text{O}_3$: C, 64.17; H, 5.15; N, 19.52. Found: C, 63.97; H, 5.19; N, 19.48.

5.27. *N*-[5-[(2-[(Cyclopropylcarbonyl)amino]imidazo[1,2-*a*]pyridin-6-yl)oxy]-2-methylphenyl]-1,3-dimethyl-1*H*-pyrazole-5-carboxamide (17b)

The compound **17b** was prepared from **15b** in a manner similar to that described for **16a** and **17a** to yield white crystals (41%): mp 265–268 °C; ^1H NMR (DMSO- d_6) δ 0.78–0.81 (4H, m), 1.91–1.94 (1H, m), 2.18 (3H, s), 2.19 (3H, s), 3.96 (3H, s), 6.78 (1H, s), 6.88 (1H, dd, J = 8.5, 2.9 Hz), 7.02–7.08 (2H, m), 7.26 (1H, d, J = 8.5 Hz), 7.46 (1H, d, J = 9.4 Hz), 8.06 (1H, s), 8.53–8.55 (1H, m), 9.74 (1H, s), 10.97 (1H, s); Anal. Calcd for $\text{C}_{24}\text{H}_{24}\text{N}_6\text{O}_3 \cdot 0.25\text{H}_2\text{O}$: C, 64.20; H, 5.50; N, 18.72. Found: C, 64.47; H, 5.63; N, 18.40.

5.28. *N*-(3-Hydroxyphenyl)-1,3-dimethyl-1*H*-pyrazole-5-carboxamide (18)

The compound **18** was prepared from 3-aminophenol and **8** in a manner similar to that described for **9a** to yield a white solid (90%): ^1H NMR (DMSO- d_6) δ 2.19 (3H, s), 3.98 (3H, s), 6.47–6.53 (1H, m), 6.79 (1H, s), 7.08–7.13 (2H, m), 7.28 (1H, s), 9.41 (1H, s), 9.97 (1H, s).

5.29. 1,3-Dimethyl-*N*-{3-[(5-nitropyridin-2-yl)oxy]phenyl}-1*H*-pyrazole-5-carboxamide (19a)

A mixture of **18** (1.58 g, 6.83 mmol), 2-chloro-5-nitropyridine (1.03 g, 6.51 mmol), potassium carbonate (1.42 g, 10.2 mmol), and DMF (10 mL) was stirred at 60 °C for 15 h. The mixture was diluted with water and extracted with AcOEt. The extract was washed with water and brine, dried over anhydrous magnesium sulfate, and concentrated under reduced pressure. The residue was purified by silica gel column chromatography (AcOEt/hexane) to give **19a** (2.26 g, 94%) as a white solid: ^1H NMR (DMSO- d_6) δ 2.20 (3H, s), 3.98 (3H, s), 6.83 (1H, s), 6.96–7.00 (1H, m), 7.28 (1H, d, J = 9.3 Hz), 7.44 (1H, t, J = 8.3 Hz), 7.58–7.62 (1H, m), 7.69 (1H, t, J = 2.1 Hz), 8.61–8.65 (1H, m), 9.04 (1H, d, J = 3.3 Hz), 10.27 (1H, s).

5.30. 1,3-Dimethyl-*N*-{2-methyl-5-[(5-nitropyridin-2-yl)oxy]phenyl}-1*H*-pyrazole-5-carboxamide (19b)

The compound **19b** was prepared from 3-aminophenol and **9a** in a manner similar to that described for **19a** to yield a white solid (94%): ^1H NMR (DMSO- d_6) δ 2.19 (3H, s), 2.25 (3H, s), 3.97 (3H, s), 6.81 (1H, s), 7.04 (1H, dd, J = 8.7, 2.9 Hz), 7.24–7.27 (2H, m), 7.35 (1H, d, J = 8.7 Hz), 8.62 (1H, dd, J = 8.9, 2.9 Hz), 9.01 (1H, dd, J = 2.7, 0.6 Hz), 9.81 (1H, s).

5.31. *N*-{3-[(5-Aminopyridin-2-yl)oxy]phenyl}-1,3-dimethyl-1*H*-pyrazole-5-carboxamide (20a)

A mixture of **19a** (2.26 g, 6.40 mmol), 10% palladium on carbon (water ~50%, 200 mg), and MeOH (20 mL) was stirred under a hydrogen atmosphere at room temperature for 5 h. The catalyst was filtered off, and the filtrate was concentrated in vacuo. The residue was collected by filtration and washed with AcOEt–hexane to give **20a** (1.77 g, 86%) as a white solid: ^1H NMR (DMSO- d_6) δ 2.19 (3H, s), 3.97 (3H, s), 5.14 (2H, s), 6.67–6.71 (1H, m), 6.76–7.00 (2H, m), 7.08 (1H, dd, J = 8.4, 3.0 Hz), 7.28 (1H, t, J = 8.1 Hz), 7.36 (1H, t, J = 2.1 Hz), 7.43–7.47 (1H, m), 7.56 (1H, d, J = 3.0 Hz), 11.10 (1H, s).

5.32. *N*-{5-[(5-Aminopyridin-2-yl)oxy]-2-methylphenyl}-1,3-dimethyl-1*H*-pyrazole-5-carboxamide (20b)

The compound **20b** was prepared from **19b** in a manner similar to that described for **20a** to yield a white solid (quant): ^1H NMR (DMSO- d_6) δ 2.17 (3H, s), 2.18 (3H, s), 3.97 (3H, s), 5.10 (2H, s), 6.74–6.80 (3H, m), 6.93 (1H, d, J = 2.7 Hz), 7.07 (1H, dd, J = 8.7, 3.0 Hz), 7.20 (1H, d, J = 9.0 Hz), 7.53–7.54 (1H, m), 9.72 (1H, s).

5.33. *N*-{3-[(2-Amino[1,3]thiazolo[5,4-*b*]pyridin-5-yl)oxy]phenyl}-1,3-dimethyl-1*H*-pyrazole-5-carboxamide (21a)

To a suspension of **20a** (1.75 g, 5.41 mmol), potassium thiocyanate (4.21 g, 43.3 mmol) in AcOH (10 mL) was added a solution of bromine (1 mL) in AcOH (4 mL) at 0 °C, and the mixture was stirred at 0 °C for 2 h and at room temperature for 15 h. Water (10 mL) was added to the mixture, and the resulting mixture was warmed to 80 °C. The resulting solid was filtrated off, and the filtrate was neutralized with 8 N NaOH. The resulting solid was collected and washed with water to give **21a** (1.05 g, 51%) as a white solid: ^1H

NMR (DMSO- d_6) δ 2.19 (3H, s), 3.98 (3H, s), 6.81–6.86 (2H, m), 6.92 (1H, d, J = 8.1 Hz), 7.35 (1H, t, J = 8.1 Hz), 7.50 (1H, t, J = 2.1 Hz), 7.57 (1H, d, J = 8.1 Hz), 7.68–7.74 (3H, m), 10.31 (1H, s).

5.34. *N*-[5-[(2-Amino[1,3]thiazolo[5,4-*b*]pyridin-5-yl)oxy]-2-methylphenyl]-1,3-dimethyl-1*H*-pyrazole-5-carboxamide (21b)

The compound **21b** was prepared from **20b** in a manner similar to that described for **21a** to yield a white solid (47%): ^1H NMR (DMSO- d_6) δ 2.19 (3H, s), 2.21 (3H, s), 3.98 (3H, s), 6.80 (1H, s), 6.88–6.94 (2H, m), 7.09 (1H, d, J = 2.4 Hz), 7.28 (1H, d, J = 8.7 Hz), 7.62 (2H, s), 7.71 (1H, dd, J = 8.4, 0.9 Hz), 9.77 (1H, s).

5.35. *N*-[3-[(2-[(Cyclopropylcarbonyl)amino][1,3]thiazolo[5,4-*b*]pyridin-5-yl)oxy]phenyl]-1,3-dimethyl-1*H*-pyrazole-5-carboxamide (22a)

The compound **22a** was prepared from **21a** in a manner similar to that described for **13a** to yield white crystals (56%): mp 225–228 °C; ^1H NMR (DMSO- d_6) δ 0.94–0.98 (4H, m), 1.96–2.05 (1H, m), 2.19 (3H, s), 3.97 (3H, s), 6.81 (1H, s), 6.89–6.94 (1H, m), 7.14 (1H, d, J = 8.9 Hz), 7.40 (1H, t, J = 8.4 Hz), 7.57–7.61 (2H, m), 8.17 (1H, d, J = 8.9 Hz), 10.20 (1H, s), 12.70 (1H, s); Anal. Calcd for $\text{C}_{22}\text{H}_{20}\text{N}_6\text{O}_3\text{S}\cdot 2\text{H}_2\text{O}$: C, 54.53; H, 4.99; N, 17.34. Found: C, 54.65; H, 4.85; N, 17.31.

5.36. *N*-[5-[(2-[(Cyclopropylcarbonyl)amino][1,3]thiazolo[5,4-*b*]pyridin-5-yl)oxy]-2-methylphenyl]-1,3-dimethyl-1*H*-pyrazole-5-carboxamide (22b)

The compound **22b** was prepared from **21b** in a manner similar to that described for **13c** to yield white crystals (66%): mp 228–231 °C; ^1H NMR (DMSO- d_6) δ 0.94–0.97 (4H, m), 1.95–2.02 (1H, m), 2.19 (3H, s), 2.24 (3H, s), 3.97 (3H, s), 6.80 (1H, s), 7.00 (1H, dd, J = 8.3, 2.6 Hz), 7.10 (1H, d, J = 8.4 Hz), 7.17 (1H, d, J = 2.4 Hz), 7.32 (1H, d, J = 8.7 Hz), 8.16 (1H, d, J = 8.4 Hz), 9.78 (1H, s), 12.68 (1H, s); Anal. Calcd for $\text{C}_{23}\text{H}_{22}\text{N}_6\text{O}_3\text{S}\cdot 0.25\text{H}_2\text{O}$: C, 59.15; H, 4.86; N, 17.99. Found: C, 58.96; H, 4.77; N, 17.90.

5.37. *tert*-Butyl [4-methyl-3-[(6-nitropyridin-3-yl)oxy]phenyl]carbamate (24a)

The compound **24a** was prepared from **23a** in a manner similar to that described for **4** to yield a colorless oil (44%): ^1H NMR (DMSO- d_6) δ 1.45 (9H, s), 2.06 (3H, s), 7.24–7.34 (3H, m), 7.45 (1H, dd, J = 9.2, 2.9 Hz), 8.32 (1H, d, J = 9.2 Hz), 8.38 (1H, d, J = 2.9 Hz), 9.50 (1H, s).

5.38. *tert*-Butyl [2-methyl-5-[(6-nitropyridin-3-yl)oxy]phenyl]carbamate (24b)

The compound **24b** was prepared from **23b** in a manner similar to that described for **4** to yield a pale yellow oil (53%): ^1H NMR (DMSO- d_6) δ 1.51 (9H, s), 2.28 (3H, s), 6.40 (1H, s), 6.72 (1H, dd, J = 8.3, 2.6 Hz), 7.20 (1H, d, J = 8.3 Hz), 7.40 (1H, dd, J = 9.0, 2.6 Hz), 7.84 (1H, d, J = 1.9 Hz), 8.22 (1H, d, J = 9.0 Hz), 8.31 (1H, d, J = 2.6 Hz).

5.39. *tert*-Butyl [3-[(6-aminopyridin-3-yl)oxy]-4-methylphenyl]carbamate (25a)

The compound **25a** was prepared from **24a** in a manner similar to that described for **5** to yield a colorless oil (99%): ^1H NMR (DMSO- d_6) δ 1.40 (9H, s), 2.16 (3H, s), 5.80 (2H, s), 6.46 (1H, d, J = 9.0 Hz), 6.89 (1H, s), 7.01–7.13 (3H, m), 7.66 (1H, d, J = 3.0 Hz), 9.50 (1H, s).

5.40. *tert*-Butyl [5-[(6-aminopyridin-3-yl)oxy]-2-methylphenyl]carbamate (25b)

The compound **25b** was prepared from **24b** in a manner similar to that described for **5** to yield a pale yellow oil (98%): ^1H NMR (DMSO- d_6) δ 1.50 (9H, s), 2.20 (3H, s), 6.30 (1H, s), 6.55 (1H, dd, J = 8.3, 2.7 Hz), 6.60 (1H, d, J = 8.7 Hz), 7.05 (1H, d, J = 8.3 Hz), 7.25–7.31 (1H, m), 7.59 (1H, s), 7.75 (1H, d, J = 2.7 Hz), 8.02 (2H, s).

5.41. *tert*-Butyl [3-[(2-amino[1,2,4]triazolo[1,5-*a*]pyridin-6-yl)oxy]-4-methylphenyl]carbamate (26a)

The compound **26a** was prepared from **25a** in a manner similar to that described for **12a** to yield a white solid (87%): ^1H NMR (DMSO- d_6) δ 1.39 (9H, s), 2.19 (3H, s), 6.00 (2H, s), 6.98 (1H, s), 7.12–7.18 (2H, m), 7.24 (1H, dd, J = 9.5, 2.3 Hz), 7.39 (1H, dd, J = 9.5, 0.3 Hz), 8.43 (1H, d, J = 1.8 Hz), 9.23 (1H, s).

5.42. *tert*-Butyl [5-[(2-amino[1,2,4]triazolo[1,5-*a*]pyridin-6-yl)oxy]-2-methylphenyl]carbamate (26b)

The compound **26b** was prepared from **25b** in a manner similar to that described for **12a** to yield a white solid (49%): ^1H NMR (CDCl_3) δ 1.50 (9H, s), 2.22 (3H, s), 4.42 (2H, s), 6.32 (1H, s), 6.61 (1H, dd, J = 8.3, 2.7 Hz), 7.09 (1H, d, J = 8.3 Hz), 7.23 (1H, d, J = 2.3 Hz), 7.32–7.38 (1H, m), 7.70 (1H, d, J = 1.9 Hz), 8.07 (1H, d, J = 1.9 Hz).

5.43. *N*-[6-(5-Amino-2-methylphenoxy)[1,2,4]triazolo[1,5-*a*]pyridin-2-yl]cyclopropanecarboxamide (27a)

To a solution of **26a** (1.50 g, 4.22 mmol) in DMA (5 mL) was added cyclopropanecarbonyl chloride (1.15 mL, 12.7 mmol) at 0 °C, and the mixture was stirred at room temperature for 2 h. The mixture was diluted with water and extracted with AcOEt. The extract was washed with water and brine, dried over anhydrous magnesium sulfate, and concentrated under reduced pressure. The residual solid was collected and washed with AcOEt–hexane to give *tert*-butyl [3-[(2-[(cyclopropylcarbonyl)amino][1,2,4]triazolo[1,5-*a*]pyridin-6-yl)oxy]-4-methylphenyl]carbamate (1.59 g, 89%) as a white solid. The solid thus obtained (1.50 g, 3.54 mmol) was dissolved in trifluoroacetic acid (5 mL), and the solution was stirred at 0 °C for 30 min. The mixture was evaporated and the residue was dissolved in water. The solution was neutralized with saturated aqueous sodium hydrogen carbonate and extracted with AcOEt. The organic layer was separated and washed with water, brine, dried over anhydrous magnesium sulfate, and concentrated under reduced pressure. The residual solid was collected and washed with AcOEt–hexane to give **27a** (1.04 g, 91%) as a white solid: ^1H NMR (DMSO- d_6) δ 0.81–0.84 (4H, m), 1.99–2.08 (1H, m), 2.09 (3H, s), 5.09 (2H, br s), 6.08 (1H, d, J = 2.1 Hz), 6.30 (1H, dd, J = 8.2, 2.1 Hz), 6.93 (1H, d, J = 8.2 Hz), 7.42 (1H, dd, J = 9.6, 2.3 Hz), 7.69 (1H, d, J = 9.6 Hz), 8.61 (1H, d, J = 2.3 Hz), 10.98 (1H, s).

5.44. *N*-[6-(3-Amino-4-methylphenoxy)[1,2,4]triazolo[1,5-*a*]pyridin-2-yl]cyclopropanecarboxamide (27b)

The compound **27b** was prepared from **26b** in a manner similar to that described for **27a** to yield a white solid (86%): ^1H NMR (CDCl_3) δ 0.87–0.97 (2H, m), 1.15–1.23 (2H, m), 1.65 (1H, s), 2.14 (3H, s), 3.70 (2H, s), 6.29–6.39 (2H, m), 7.01 (1H, d, J = 7.5 Hz), 7.33–7.41 (1H, m), 7.55 (1H, dd, J = 9.8, 0.8 Hz), 8.27 (1H, d, J = 1.9 Hz), 9.56 (1H, s).

5.45. *N*-[3-({2-[(Cyclopropylcarbonyl)amino][1,2,4]triazolo[1,5-*a*]pyridin-6-yl}oxy)-4-methylphenyl]-1,3-dimethyl-1*H*-pyrazole-5-carboxamide (28)

To a solution of **27a** (265 mg, 0.820 mmol) in DMA (5 mL) was added a solution of 1,3-dimethyl-1*H*-pyrazole-5-carbonyl chloride (260 mg, 1.64 mmol) dropwise at 0 °C, and the mixture was stirred at room temperature for 15 h. The mixture was diluted with water and extracted with AcOEt. The extract was washed with brine, dried over anhydrous magnesium sulfate, and concentrated under reduced pressure. The residue was purified by silica gel column chromatography (AcOEt/hexane) followed by recrystallization from AcOEt to give **28** (333 mg, 91%) as white crystals: mp 222–225 °C; ¹H NMR (DMSO-*d*₆) δ 0.81–0.84 (4H, m), 1.99–2.08 (1H, m), 2.15 (3H, s), 2.27 (3H, s), 3.93 (3H, s), 6.72 (1H, s), 7.21–7.30 (2H, m), 7.48–7.56 (2H, m), 7.74 (1H, dd, *J* = 9.5, 0.7 Hz), 8.78–8.80 (1H, m), 10.02 (1H, s), 11.04 (1H, s); Anal. Calcd for C₂₃H₂₃N₇O₃·0.5H₂O: C, 60.78; H, 5.32; N, 21.57. Found: C, 61.04; H, 5.29; N, 21.55.

5.46. *N*-[5-({2-[(Cyclopropylcarbonyl)amino][1,2,4]triazolo[1,5-*a*]pyridin-6-yl}oxy)-2-methylphenyl]-2,5-dimethyl-1,3-thiazole-4-carboxamide (29a)

To a solution of 2,5-dimethyl-1,3-thiazole-4-carboxylic acid (107 mg, 0.681 mmol) in THF (5 mL) was added thionyl chloride (118 μL, 1.36 mmol) and two drops of DMF. The mixture was stirred at room temperature for 2 h and concentrated under reduced pressure. The residue was dissolved in DMA (6 mL), and **27b** (200 mg, 0.619 mmol) was added to the solution at 0 °C. The mixture was stirred at room temperature for 2 h. The mixture was diluted with saturated aqueous sodium hydrogen carbonate and extracted with AcOEt. The extract was washed with saturated aqueous sodium hydrogen carbonate, brine, dried over anhydrous magnesium sulfate, and concentrated under reduced pressure. The residual solid was recrystallized from EtOH to give **29a** (248 mg, 87%) as white crystals: mp 239–240 °C; ¹H NMR (DMSO-*d*₆) δ 0.78–0.86 (4H, m), 2.04 (1H, br s), 2.23–2.28 (3H, m), 2.65 (3H, s), 2.70 (3H, s), 6.82 (1H, dd, *J* = 8.3, 2.7 Hz), 7.27 (1H, d, *J* = 8.7 Hz), 7.50 (1H, dd, *J* = 9.5, 2.3 Hz), 7.66 (1H, d, *J* = 2.7 Hz), 7.69–7.75 (1H, m), 8.82 (1H, dd, *J* = 2.3, 0.8 Hz), 9.66 (1H, s), 11.02 (1H, s); Anal. Calcd for C₂₃H₂₂N₆O₃S: C, 59.73; H, 4.79; N, 18.17. Found: C, 59.48; H, 4.80; N, 18.00.

The following compounds **29b–f** were prepared from **27b** using a procedure similar to that described for **29a**.

5.47. *N*-[5-({2-[(Cyclopropylcarbonyl)amino][1,2,4]triazolo[1,5-*a*]pyridin-6-yl}oxy)-2-methylphenyl]-3-chloro-4-methylthiophene-2-carboxamide (29b)

Yield 78%, pale yellow crystals: mp 218–219 °C; ¹H NMR (DMSO-*d*₆) δ 0.79–0.86 (4H, m), 2.04 (1H, br s), 2.20 (3H, d, *J* = 1.1 Hz), 2.27 (3H, s), 6.89 (1H, dd, *J* = 8.3, 2.6 Hz), 7.28 (1H, d, *J* = 8.7 Hz), 7.42 (1H, d, *J* = 2.6 Hz), 7.50 (1H, dd, *J* = 9.8, 2.7 Hz), 7.66 (1H, d, *J* = 1.1 Hz), 7.69–7.76 (1H, m), 8.84 (1H, dd, *J* = 2.3, 0.8 Hz), 9.54 (1H, s), 10.96–11.09 (1H, m); Anal. Calcd for C₂₃H₂₀ClN₅O₃S: C, 57.32; H, 4.18; N, 14.53. Found: C, 57.28; H, 4.04; N, 14.51.

5.48. *N*-[5-({2-[(Cyclopropylcarbonyl)amino][1,2,4]triazolo[1,5-*a*]pyridin-6-yl}oxy)-2-methylphenyl]-1,3-dimethyl-1*H*-pyrazole-4-carboxamide (29c)

Yield 58%, pale brown crystals: mp 192–194 °C; ¹H NMR (DMSO-*d*₆) δ 0.79–0.86 (4H, m), 2.04 (1H, br s), 2.20 (3H, s), 2.32

(3H, s), 3.79 (3H, s), 6.86 (1H, dd, *J* = 8.5, 2.8 Hz), 7.17 (1H, d, *J* = 2.6 Hz), 7.25 (1H, d, *J* = 8.7 Hz), 7.49 (1H, dd, *J* = 9.6, 2.5 Hz), 7.72 (1H, dd, *J* = 9.4, 0.8 Hz), 8.23 (1H, s), 8.81 (1H, dd, *J* = 2.3, 0.8 Hz), 9.16 (1H, s), 11.03 (1H, s); Anal. Calcd for C₂₃H₂₃N₇O₃·0.5H₂O: C, 60.78; H, 5.31; N, 21.57. Found: C, 61.20; H, 5.76; N, 19.77.

5.49. *N*-[5-({2-[(Cyclopropylcarbonyl)amino][1,2,4]triazolo[1,5-*a*]pyridin-6-yl}oxy)-2-methylphenyl]-1-methyl-1*H*-pyrazole-5-carboxamide (29d)

Yield 47%, white crystals: mp 131–135 °C; ¹H NMR (DMSO-*d*₆) δ 0.78–0.87 (4H, m), 2.04 (1H, br s), 2.20 (3H, s), 4.05 (3H, s), 6.94 (1H, dd, *J* = 8.3, 2.7 Hz), 7.02 (1H, d, *J* = 1.9 Hz), 7.09 (1H, d, *J* = 2.7 Hz), 7.29 (1H, d, *J* = 8.7 Hz), 7.46–7.53 (2H, m), 7.72 (1H, dd, *J* = 9.8, 0.8 Hz), 8.82–8.85 (1H, m), 9.86 (1H, s), 11.02 (1H, s); Anal. Calcd for C₂₂H₂₁N₇O₃: C, 61.24; H, 4.91; N, 22.73. Found: C, 61.24; H, 4.98; N, 22.58.

5.50. *N*-[5-({2-[(Cyclopropylcarbonyl)amino][1,2,4]triazolo[1,5-*a*]pyridin-6-yl}oxy)-2-methylphenyl]-2-methylpropanecarboxamide (29e)

Yield 72%, white crystals: mp 217–219 °C; ¹H NMR (DMSO-*d*₆) δ 0.79–0.85 (4H, m), 0.93 (6H, d, *J* = 6.4 Hz), 1.96–2.11 (2H, m), 2.16–2.23 (5H, m), 6.79 (1H, dd, *J* = 8.3, 2.7 Hz), 7.17–7.25 (2H, m), 7.47 (1H, dd, *J* = 9.7, 2.5 Hz), 7.71 (1H, dd, *J* = 9.5, 0.8 Hz), 8.79 (1H, dd, *J* = 2.3, 0.8 Hz), 9.21 (1H, s), 11.01 (1H, s); Anal. Calcd for C₂₂H₂₅N₅O₃: C, 64.85; H, 6.18; N, 17.19. Found: C, 64.71; H, 6.23; N, 17.24.

5.51. *N*-[5-({2-[(Cyclopropylcarbonyl)amino][1,2,4]triazolo[1,5-*a*]pyridin-6-yl}oxy)-2-methylphenyl]cyclobutanecarboxamide (29f)

Yield 45%, white crystals: mp 229–230 °C; ¹H NMR (DMSO-*d*₆) δ 0.78–0.87 (4H, m), 1.72–1.85 (1H, m), 1.85–1.98 (1H, m), 1.98–2.14 (3H, m), 2.15 (3H, s), 2.17–2.27 (2H, m), 3.21–3.35 (1H, m), 6.80 (1H, dd, *J* = 8.3, 2.7 Hz), 7.20 (1H, d, *J* = 8.7 Hz), 7.25 (1H, d, *J* = 1.9 Hz), 7.47 (1H, dd, *J* = 9.5, 2.3 Hz), 7.66–7.74 (1H, m), 8.76–8.80 (1H, m), 9.05 (1H, s), 11.01 (1H, s); Anal. Calcd for C₂₂H₂₃N₅O₃: C, 65.17; H, 5.72; N, 17.27. Found: C, 65.24; H, 5.70; N, 17.34.

5.52. *N*-(6-Hydroxy-1,3-benzothiazol-2-yl)cyclopropanecarboxamide (31)

To a solution of **30** (9.03 g, 54.3 mmol), triethylamine (8.27 mL, 59.7 mmol) in THF (100 mL) was added a solution of cyclopropanecarbonyl chloride (5.19 mL, 57.0 mmol) in THF (25 mL) at 0 °C, and the mixture was stirred at room temperature for 2 h. The mixture was diluted with water and extracted with AcOEt. The extract was washed with water and brine, dried over anhydrous magnesium sulfate, and concentrated under reduced pressure. The residual solid was collected and washed with AcOEt–hexane to give **31** (12.3 g, 97%) as a white solid: ¹H NMR (DMSO-*d*₆) δ 0.95–1.05 (4H, m), 1.84–1.99 (1H, m), 6.93 (1H, dd, *J* = 8.8, 2.6 Hz), 7.29 (1H, d, *J* = 8.8 Hz), 7.45–7.50 (3H, m).

5.53. *N*-[6-(3-Nitrophenoxy)-1,3-benzothiazol-2-yl]cyclopropanecarboxamide (32)

A mixture of **31** (3.54 g, 15.1 mmol), 1-fluoro-3-nitrobenzene (2.24 g, 15.9 mmol), potassium carbonate (6.26 g, 45.3 mmol), and DMF (30 mL) was stirred at 150 °C for 15 h. The mixture was diluted with water and extracted with AcOEt. The extract was washed with water and brine, dried over anhydrous magnesium

sulfate, and concentrated under reduced pressure. The residual solid was collected and washed with AcOEt–hexane to give **32** (1.82 g, 37%) as a white solid: ^1H NMR (DMSO- d_6) δ 0.95–0.99 (4H, m), 1.96–2.05 (1H, m), 7.24 (1H, dd, J = 8.7, 2.7 Hz), 7.47–7.51 (1H, m), 7.63–7.70 (2H, m), 7.78–7.83 (2H, m), 7.94–7.99 (1H, m), 12.67 (1H, s).

5.54. *N*-[3-({2-[(Cyclopropylcarbonyl)amino]-1,3-benzothiazol-6-yl}oxy)phenyl]-1,3-dimethyl-1*H*-pyrazole-5-carboxamide (**33**)

A mixture of **32** (1.80 g, 5.53 mmol), 10% palladium on carbon (water ~50%, 100 mg), and MeOH (20 mL) was stirred under a hydrogen atmosphere at room temperature for 5 h. The catalyst was filtered off, and the filtrate was concentrated in vacuo. To the residue thus obtained was added iron (309 mg), calcium chloride (613 mg, 5.53 mmol), EtOH (10 mL), and water (2 mL). The mixture was stirred for 2 h. The mixture was filtered, and the filtrate was diluted with water and extracted with AcOEt. The organic layer was separated and washed with water and brine, dried over anhydrous magnesium sulfate, and concentrated under reduced pressure. The residue was dissolved in THF (10 mL), and triethylamine (192 μL , 1.39 mmol), **8** (220 mg, 1.39 mmol) were added to the solution at 0 °C. The mixture was stirred at room temperature for 3 h. The mixture was diluted with water and extracted with AcOEt. The extract was washed with water and brine, dried over anhydrous magnesium sulfate, and concentrated under reduced pressure. The residue was purified by silica gel column chromatography (AcOEt/hexane) followed by recrystallization from AcOEt–THF to give **33** (126 mg, 5.1%) as white crystals: mp 192–194 °C; ^1H NMR (DMSO- d_6) δ 0.94–0.97 (4H, m), 1.96–2.05 (1H, m), 2.17 (3H, s), 3.95 (3H, s), 6.76–6.80 (2H, m), 7.15 (1H, dd, J = 8.6, 2.6 Hz), 7.34 (1H, t, J = 8.1 Hz), 7.40 (1H, t, J = 2.3 Hz), 7.51–7.56 (1H, m), 7.70–7.77 (2H, m), 10.13 (1H, s), 12.62 (1H, s); Anal. Calcd for $\text{C}_{23}\text{H}_{21}\text{N}_5\text{O}_3\text{S}$: C, 61.73; H, 4.73; N, 15.65. Found: C, 61.49; H, 4.52; N, 15.67.

5.55. Measurement of inhibitory activities against VEGFR2, PDGFR β and FGFR1

Kinase activities of VEGFR2, PDGFR β and fibroblast growth factor receptor 1 (FGFR1) were determined by use of an anti-phosphotyrosine antibody with quantitation performed through the AlphaScreen[®] system (PerkinElmer, USA). For VEGFR2, enzyme reactions were performed in 50 mM Tris–HCl pH 7.5, 5 mM MnCl_2 , 5 mM MgCl_2 , 0.01% Tween-20 and 2 mM DTT, containing 10 μM ATP, 0.1 $\mu\text{g}/\text{mL}$ biotinylated poly-GluTyr (4:1) and 0.1 nM of VEGFR2 (Millipore, UK). For PDGFR β , kinase assay was performed as described above with 0.8 nM of PDGFR β (Millipore) and 20 μM of ATP. For FGFR1, kinase assay was performed as described above with 0.1 nM of FGFR1 (ProKinase GmbH, Germany) and 0.2 μM of ATP.

Prior to the catalytic initiation with ATP, compound and enzyme were incubated for 5 min at room temperature. The reactions were quenched by the addition of 25 μL of 100 mM EDTA, 10 $\mu\text{g}/\text{mL}$ AlphaScreen streptavidine donor beads and 10 $\mu\text{g}/\text{mL}$ acceptor beads in 62.5 mM HEPES pH7.4, 250 mM NaCl, and 0.1% BSA. Plates were incubated in the dark overnight and then read by EnVision 2102 Multilabel Reader (PerkinElmer). Wells containing the substrate and the enzyme without the compound was used as total reaction control. Wells containing the biotinylated poly-GluTyr (4:1) and the enzyme without ATP were used as basal control. The concentration of inhibitor producing 50% inhibition of the kinase activities of VEGFR2, PDGFR β and FGFR1 (IC_{50} values) and 95% confidence intervals (95% CI) were analyzed using GraphPad Prism version 5.01, GraphPad Software (USA). Sigmoidal dose–response (variable slope) curves were fitted using non-linear regres-

sion analysis, with the top and bottom of the curve constrained at 100 and 0, respectively.

5.56. Dilution assay of VEGFR2–13d complex

To test the dissociation kinetics of compounds an enzyme–inhibitor dilution assay was performed.^{29,42} The recovery of enzyme activity from a preformed enzyme–inhibitor complex was measured using the AlphaScreen[®] system as described above. VEGFR2 at 100-fold higher concentration than the standard reaction condition and **13d** at 10-fold higher concentration than IC_{50} value were incubated together in reaction buffer for 60 min at ambient temperature to form enzyme–inhibitor complex. This complex was diluted 1:100 into reaction buffer containing 1 mM ATP and 0.1 $\mu\text{g}/\text{mL}$ biotinylated poly-Glu-Tyr (4:1), to initiate the kinase reaction.

5.57. Kinase profiling by IC_{50} measurement

Kinase profiling was performed as described previously.⁴³ Briefly, kinase activities of VEGFR1, PDGFR α , Tie-2, Insulin Receptor (IR), insulin-like growth factor 1 receptor (IGF1-R), c-kit, Src and focal adhesion kinase (FAK) were determined by use of the AlphaScreen[®] system. For VEGFR1, kinase assay was performed with 20 ng/mL VEGFR1 (Millipore) and 0.5 μM ATP. For IGF1-R, kinase assay was performed with 10 ng/mL IGF1R (BIOMOL, USA) and 10 μM ATP. For FAK, kinase assay was performed with 62 ng/mL FAK (N-terminal FLAG-tagged recombinant proteins using the baculovirus expression system) and 2 μM of ATP. In these assays, wells containing the substrate and the enzyme without the compound were used as total reaction control. Wells containing the biotinylated poly-GluTyr (4:1) and the enzyme without ATP were used as basal control. Kinase activities of B-raf, extracellular signal-regulated kinases (ERK1), protein kinase C θ (PKC θ), glycogen synthase kinase-3 β (GSK3 β) and Aurora A were determined by use of radio labeled [γ - ^{33}P] ATP (GE Healthcare, USA). For GSK3 β , kinase assay was performed with 2 $\mu\text{g}/\text{mL}$ GSK3 β , 4 $\mu\text{g}/\text{well}$ of pGS peptide and 0.5 μM ATP (0.1 $\mu\text{Ci}/50 \mu\text{L}/\text{well}$ of [γ - ^{33}P] ATP). For Aurora A, kinase assay was performed with 10 $\mu\text{g}/\text{mL}$ Aurora A, 30 $\mu\text{mol}/\text{L}$ Aurora substrate peptide and 0.5 μM ATP (0.2 $\mu\text{Ci}/50 \mu\text{L}/\text{well}$ of [γ - ^{33}P] ATP). EGFR and HER2 kinase activity was determined by use of radio labeled [γ - ^{32}P] ATP (GE Healthcare). In these assays, wells containing the substrate and the enzyme without the compound were used as total reaction control. Wells containing the substrate and the radio labeled ATP without the enzyme was used as basal control. The concentration of inhibitor producing 50% inhibition of the kinase activities (IC_{50} values) and 95% confidence intervals (95% CI) were analyzed as described above.

5.58. Cell proliferation assays

HUVECs (Cambrex, USA) were seeded into a 96-well plate at 3000 cells/well in Human Endothelial-SFM Growth Medium (Invitrogen, USA) containing 3% fetal bovine serum (FBS) (Hyclone, USA) and were incubated overnight at 37 °C in a 5% CO_2 incubator. Various concentrations of the test compounds were added in the presence of 60 ng/mL VEGF (R&D systems, USA), and the cells were cultured for a further 5 days. The cellular proliferation was determined by the WST-8 formazan assay using Cell Counting Kit-8 (DOJINDO Laboratories, Japan). Briefly, 10 $\mu\text{L}/\text{well}$ of Cell Counting Kit-8 was added and the cells were cultured for several hours. Then, the absorbance value at 450 nm was measured using a Benchmark Plus Microplatereader (Bio-Rad Labs., USA). The IC_{50} values and 95% confidence intervals (95% CI) were calculated from a dose–response curve generated by least-squares linear regression

of the response using NLIN procedure of the SAS software (SAS Institute Japan, Inc., Japan).

5.59. Pharmacokinetic studies

Test compounds were administered at a dose of 10 mg/kg by cassette dosing to nonfasted mice. After oral administration, blood samples were collected. The blood samples were centrifuged to obtain the plasma fraction. The plasma samples were deproteinized with acetonitrile containing an internal standard. After centrifugation, the supernatant was diluted with a mixture of 0.01 mol/L ammonium formate solution and acetonitrile (9:1, v/v) and centrifuged again. The compound concentrations in the supernatant were measured by LC/MS/MS.

5.60. In vivo tumor growth inhibition model

Human prostate carcinoma cell line DU145 (ATCC No. HTB-81) and human lung carcinoma cell line A549 (ATCC No. CCL-185) were obtained from American Type Culture Collection (USA). The cells were proliferated in DMEM (Invitrogen, USA) supplemented with 10% heat-inactivated fetal bovine serum (HyClone, USA) and antibiotics (100 units/mL penicillin G and 100 µg/mL streptomycin, Wako Pure Chemical, Japan). The cells were cultured in tissue culture dishes in a humidified incubator at 37 °C in an atmosphere of 5% CO₂ and 95% air. Compound was suspended in 0.5 w/v % methylcellulose (Shin-Etsu Chemical, Japan) vehicle solution.

Six-week old male athymic nude mice (BALB/cA Jcl-nu/nu, Japan Clea, Japan) received subcutaneous injections into the hind flank with 2.5×10^6 DU145 cells in 100 µL of 1:1 volume mixture of Hanks' balanced salt solution (Invitrogen) and Matrigel (BD Biosciences, USA) or 5×10^6 A549 cells in 100 µL of Hanks' balanced salt solution. When tumors reached a volume of 110–210 mm³ (DU145) and 90–130 mm³ (A549), mice were randomized into groups of 4 ($n = 6$ (DU145), $n = 5$ (A549)). Then mice were orally given vehicle (0.5% w/v methylcellulose (Shin-Etsu Chemical, Japan) or **13d** twice-daily for 2 weeks. Compound **13d** was administered at doses of 0.5, 1.5, and 5 mg/kg.

Tumor volumes were assessed by bilateral vernier caliper measurement twice-weekly after inoculation and calculated using the formula $\text{length} \times \text{width}^2 \times 1/2$, where length was taken to be the longest diameter across the tumor and width the corresponding perpendicular. Treatment per control (T/C , %), an index of antitumor efficacy, was calculated by comparison of the mean change in tumor volume over the treatment period for the control and treated groups. Body weight was also measured on the day of tumor volume assessment. Effect of compound **13d** on tumor growth and body weight was statistically analyzed by a one-tailed Williams' test. Differences were considered significant at $p \leq 0.025$.

Acknowledgements

The authors thank Ms. T. Yoshida, Ms. Y. Awazu, Dr. A. Mizutani, and Mr. Y. Nagase for in vitro and in vivo assays. The authors thank Mr. S. Yamasaki and Ms. Y. Watanabe for PK evaluation and Dr. T. Kitazaki for helpful discussion.

References and notes

- Folkman, J. *N. Engl. J. Med.* **1971**, *285*, 1182.
- Ferrara, N.; Kerbel, R. S. *Nature* **2005**, *438*, 967.
- Olsson, A. K.; Dimberg, A.; Kreuger, J.; Claesson-Welsh, L. *Nat. Rev. Mol. Cell Biol.* **2006**, *7*, 359.
- Rak, J.; Mitsunashi, Y.; Bayko, L.; Filmus, J.; Shirasawa, S.; Sasazuki, T.; Kerbel, R. S. *Cancer Res.* **1995**, *55*, 4575.
- Zhang, L.; Yu, D.; Hu, M.; Xiong, S.; Lang, A.; Ellis, L. M.; Pollock, R. E. *Cancer Res.* **2000**, *60*, 3655.
- Mukhopadhyay, D.; Knebelmann, B.; Cohen, H. T.; Ananth, S.; Sukhatme, V. P. *Mol. Cell. Biol.* **1997**, *17*, 5629.
- Ferrara, N.; Gerber, H. P.; LeCouter, J. *Nat. Med.* **2003**, *9*, 669.
- Forsythe, J. A.; Jiang, B. H.; Iyer, N. V.; Agani, F.; Leung, S. W.; Koos, R. D.; Semenza, G. L. *Mol. Cell. Biol.* **1996**, *16*, 4604.
- Shweiki, D.; Itin, A.; Soffer, D.; Keshet, E. *Nature* **1992**, *359*, 843.
- De Vries, C.; Escobedo, J. A.; Ueno, H.; Houck, K.; Ferrara, N.; Williams, L. T. *Science* **1992**, *255*, 989.
- Waltenberger, J.; Claesson-Welsh, L.; Siegbahn, A.; Shibuya, M.; Heldin, C. H. *J. Biol. Chem.* **1994**, *269*, 26988.
- Kaipainen, A.; Korhonen, J.; Mustonen, T.; van Hinsbergh, V. W.; Fang, G. H.; Dumont, D.; Breitman, M.; Alitalo, K. *Proc. Nat. Acad. Sci. U.S.A.* **1995**, *92*, 3566.
- Rahimi, N. *Exp. Eye Res.* **2006**, *83*, 1005.
- Poon, R. T.; Fan, S. T.; Wong, J. *J. Clin. Oncol.* **2001**, *19*, 1207.
- Takahashi, Y.; Kitada, Y.; Bucana, C. D.; Cleary, K. R.; Ellis, L. M. *Cancer Res.* **1995**, *55*, 3964.
- Motzer, R. J.; Michaelson, M. D.; Redman, B. G.; Hudes, G. R.; Wilding, G.; Figlin, R. A.; Ginsberg, M. S.; Kim, S. T.; Baum, C. M.; DePrimo, S. E.; Li, J. Z.; Bello, C. L.; Theuer, C. P.; George, D. J.; Rini, B. I. *J. Clin. Oncol.* **2006**, *24*, 16.
- Strumberg, D. *Drugs Today* **2005**, *41*, 773.
- Harris, P. A.; Bolor, A.; Cheung, M.; Kumar, R.; Crosby, R. M.; Davis-Ward, R. G.; Epperly, A. H.; Hinkle, K. W.; Hunter, R. N. I. I.; Johnson, J. H.; Knick, V. B.; Laudeman, C. P.; Luttrell, D. K.; Mook, R. A.; Nolte, R. T.; Rudolph, S. K.; Szweczyk, J. R.; Truesdale, A. T.; Veal, J. M.; Wang, L.; Stafford, J. A. *J. Med. Chem.* **2008**, *51*, 4632.
- Rini, B. I.; Escudier, B.; Tomczak, P.; Kaprin, A.; Szczylak, C.; Hutson, T. E.; Michaelson, M. D.; Gorbunova, V. A.; Gore, M. E.; Rusakov, I. G.; Negrier, S.; Ou, Y. C.; Castellano, D.; Lim, H. Y.; Uemura, H.; Tarazi, J.; Cella, D.; Chen, C.; Rosbrook, B.; Kim, S.; Motzer, R. J. *Lancet* **1991**, *337*, 378.
- Strumberg, D.; Scheulen, M. E.; Schultheis, B.; Richly, H.; Frost, A.; Büchert, M.; Christensen, O.; Jeffers, M.; Heinig, R.; Boix, O.; Mross, K. *Br. J. Cancer* **2012**, *106*, 1722.
- Liu, Y.; Gray, N. S. *Nat. Chem. Biol.* **2006**, *2*, 358.
- Pargellis, C.; Tong, L.; Churchill, L.; Cirillo, P. F.; Gilmore, T.; Graham, A. G.; Grob, P. M.; Hickey, E. R.; Moss, N.; Pav, S.; Regan, J. *Nat. Struct. Biol.* **2002**, *9*, 268.
- Fabian, M. A.; Biggs, W. H., III; Treiber, D. K.; Atteridge, C. E.; Azimioara, M. D.; Benedetti, M. G.; Carter, T. A.; Ciceri, P.; Edeen, P. T.; Floyd, M.; Ford, J. M.; Galvin, M.; Gerlach, J. L.; Grotzfeld, R. M.; Herrgard, S.; Insko, D. E.; Insko, M. A.; Lai, A. G.; Lélias, J. M.; Mehta, S. A.; Milanov, Z. V.; Velasco, A. M.; Wodicka, L. M.; Patel, H. K.; Zarrinkar, P. P.; Lockhart, D. J. *Nat. Biotechnol.* **2005**, *23*, 329.
- Oguro, Y.; Miyamoto, N.; Okada, K.; Takagi, T.; Iwata, H.; Awazu, Y.; Miki, H.; Hori, A.; Kamiyama, K.; Imamura, S. *Bioorg. Med. Chem.* **2010**, *18*, 7260.
- Miyamoto, N.; Sakai, N.; Hirayama, T.; Miwa, K.; Oguro, Y.; Oki, H.; Okada, K.; Takagi, T.; Iwata, H.; Awazu, Y.; Yamasaki, S.; Takeuchi, T.; Miki, H.; Hori, A.; Imamura, S. *Bioorg. Med. Chem.* **2013**, *21*, 2333.
- Nettekoven, M.; Pullmann, B.; Schmitt, S. *Synthesis* **2003**, *11*, 1649.
- Bochis, R. J.; Olen, L. E.; Fisher, M. H.; Reamer, R. A.; Wilks, G.; Taylor, J. E.; Olson, G. *J. Med. Chem.* **1981**, *24*, 1483.
- Okafor, C. O. *J. Org. Chem.* **1973**, *38*, 4383.
- Ullman, E. F.; Kirakossian, H.; Singh, S.; Wu, Z. P.; Irvin, B. R.; Pease, J. S.; Switchenko, A. C.; Irvine, J. D.; Dafforn, A.; Skold, C. N.; Wagner, D. B. *Proc. Natl. Acad. Sci. U.S.A.* **1994**, *91*, 5426.
- Mol, C. D.; Dougan, D. R.; Schneider, T. R.; Skene, R. J.; Kraus, M. L.; Scheibe, D. N.; Snell, G. P.; Zou, H.; Sang, B. C.; Wilson, K. P. *J. Biol. Chem.* **2004**, *279*, 31655.
- Heron, N. M.; Anderson, M.; Blowers, D. P.; Breed, J.; Eden, J. M.; Green, S.; Hill, G. B.; Johnson, T.; Jung, F. H.; McMiken, H. H.; Mortlock, A. A.; Pannifer, A. D.; Pauptit, R. A.; Pink, J.; Roberts, N. J.; Rowsell, S. *Bioorg. Med. Chem. Lett.* **2006**, *16*, 1320.
- Wan, P. T.; Garnett, M. J.; Roe, S. M.; Lee, S.; Niculescu-Duvaz, D.; Good, V. M.; Jones, C. M.; Marshall, C. J.; Springer, C. J.; Barford, D.; Marais, R. *Cell* **2004**, *116*, 855.
- Hodous, B. L.; Geuns-Meyer, S. D.; Hughes, P. E.; Albrecht, B. K.; Bellon, S.; Bready, J.; Caenepeel, S.; Cee, V. J.; Chaffee, S. C.; Coxon, A.; Emery, M.; Fretland, J.; Gallant, P.; Gu, Y.; Hoffman, D.; Johnson, R. E.; Kendall, R.; Kim, J. L.; Long, A. M.; Morrison, M.; Olivieri, P. R.; Patel, V. F.; Polverino, A.; Rose, P.; Tempest, P.; Wang, L.; Whittington, D. A.; Zhao, H. *J. Med. Chem.* **2007**, *50*, 611.
- Yalkowsky, S. H.; Banerjee, S. *Aqueous Solubility, Methods of Estimation for Organic Compounds*; Marcel Dekker: New York, Basel and Hong Kong, 1992. pp 128–148.
- Nagao, Y.; Hirata, T.; Goto, S.; Sano, S.; Kakehi, A.; Iizuka, K.; Shiro, M. *J. Am. Chem. Soc.* **1998**, *120*, 3104.
- Ishikawa, M.; Hashimoto, Y. *J. Med. Chem.* **2011**, *54*, 1539.
- Iwata, H.; Imamura, S.; Hori, A.; Hixon, M. S.; Kimura, H.; Miki, H. *Bioorg. Med. Chem.* **2011**, *19*, 5342.
- Iwata, H.; Imamura, S.; Hori, A.; Hixon, M. S.; Kimura, H.; Miki, H. *Biochemistry* **2011**, *50*, 738.
- Copeland, R. A.; Pompliano, D. L.; Meek, T. D. *Nat. Rev. Drug Disc.* **2006**, *5*, 730.
- Abramsson, A.; Lindblom, P.; Betsholtz, C. *J. Clin. Invest.* **2003**, *112*, 1142.
- Bergers, G.; Song, S.; Meyer-Morse, N.; Bergsland, E.; Hanahan, D. *J. Clin. Invest.* **2003**, *111*, 1287.
- Copeland, R. A. *Methods Biochem. Anal.* **2005**, *46*, 1.
- Saitoh, M.; Kunitomo, J.; Kimura, E.; Hayase, Y.; Kobayashi, H.; Uchiyama, N.; Kawamoto, T.; Tanaka, T.; Mol, C. D.; Dougan, D. R.; Textor, G. S.; Snell, G. P.; Itoh, F. *Bioorg. Med. Chem.* **2009**, *17*, 2017.